Progress in direct measurements of the Hubble constant

Journal of Cosmology and Astroparticle Physics
An IOP and SISSA journal

Received: *September 19, 2023*
Revised: *October 19, 2023*
Accepted: *October 23, 2023*
Published: *November 10, 2023*

JCAP Anniversary Special Issue

Progress in direct measurements of the Hubble constant

Wendy L. Freedman[a] **and Barry F. Madore**[b,c]

[a]*The Department of Astronomy & Astrophysics, and the Kavli Institute for Cosmological Physics, University of Chicago, 5640 S. Ellis Ave., Chicago, IL 60637, U.S.A.*
[b]*The Observatories, Carnegie Institution for Science, 813 Santa Barbara St., Pasadena, CA 91101, U.S.A.*
[c]*Department of Astronomy & Astrophysics, University of Chicago, 5640 S. Ellis Ave., Chicago, IL 60637, U.S.A.*

E-mail: wfreedman@uchicago.edu, barry.f.madore@gmail.com

Abstract: One of the most exciting and pressing issues in cosmology today is the discrepancy between some measurements of the local Hubble constant and other values of the expansion rate inferred from the observed temperature and polarization fluctuations in the cosmic microwave background (CMB) radiation. Resolving these differences holds the potential for the discovery of new physics beyond the standard model of cosmology: Lambda Cold Dark Matter (ΛCDM), a successful model that has been in place for more than 20 years. Given both the fundamental significance of this outstanding discrepancy, and the many-decades-long effort to increase the accuracy of the extragalactic distance scale, it is critical to demonstrate that the local measurements are convincingly free from residual systematic errors. We review the progress over the past quarter century in measurements of the local value of the Hubble constant, and discuss remaining challenges. Particularly exciting are new data from the James Webb Space Telescope (*JWST*), for which we present an overview of our program and first results. We focus in particular on Cepheids and the Tip of the Red Giant Branch (TRGB) stars, as well as a relatively new method, the JAGB (J-Region Asymptotic Giant Branch) method, all methods that currently exhibit the demonstrably smallest statistical and systematic uncertainties. *JWST* is delivering high-resolution near-infrared imaging data to both test for and to address directly several of the systematic uncertainties that have historically limited the accuracy of extragalactic distance scale measurements (e.g., the dimming effects of interstellar dust, chemical composition differences in the atmospheres of stars, and the crowding and blending of Cepheids contaminated by nearby previously

https://doi.org/10.1088/1475-7516/2023/11/050

JCAP11(2023)050

unresolved stars). For the first galaxy in our program, NGC 7250, the high-resolution *JWST* images demonstrate that many of the Cepheids observed with the Hubble Space Telescope (HST) are significantly crowded by nearby neighbors. Avoiding the more significantly crowded variables, the scatter in the *JWST* near-infrared (NIR) Cepheid PL relation is decreased by a factor of two compared to those from HST, illustrating the power of *JWST* for improvements to local measurements of H_0. Ultimately, these data will either confirm the standard model, or provide robust evidence for the inclusion of additional new physics.

KEYWORDS: cosmological parameters from CMBR, gravitational waves / experiments, stars, supernova type Ia - standard candles

ARXIV EPRINT: 2309.05618

JCAP11(2023)050

Contents

JCAP11(2023)050

1 Introduction

The year 2023 marks 100 years since Edwin Hubble's famous discovery of a single Cepheid variable in the Andromeda galaxy. Hubble's subsequent measurements of extragalactic distances were based (in part) on the Cepheid Period-Luminosity (PL) relation, aka the Leavitt Law [1]. Correlating these distances with spectral measurements of radial (line-of-sight) velocities [2], ultimately led to the discovery of the expansion of the universe in 1929 [3], and ushered in modern cosmology.[1]

At the time of its launch in 1990, one of the highest priorities for the Hubble Space Telescope (HST) was to convincingly measure the current rate of the expansion of the universe, the Hubble constant (H_0), to an accuracy of 10%. In a Cepheid-based calibration, the Hubble Key Project team in 2001 obtained a value of $H_0 = 72 \pm 3$ (statistical) $\pm$ 7 (systematic) [5] (see figure 1). Two additional decades of effort with HST, *Spitzer*, and many additional ground-based telescopes, subsequently improved the measurements of H_0, with estimated accuracies currently falling in the 2–5% range [6]. The Cepheid calibration of H_0 [7–9] continues to yield values of $H_0 \sim 73$ or $74\,\mathrm{km\,s^{-1}\,Mpc^{-1}}$, whereas measurements using the tip of the red giant branch (TRGB) [10–13] yield slightly lower values, closer to $70–72\,\mathrm{km\,s^{-1}\,Mpc^{-1}}$. Recent estimates of H_0 from CMB measurements have extremely high precision, with results from the Planck satellite [14] yielding $H_0 = 67.4 \pm 0.5\,\mathrm{km\,s^{-1}\,Mpc^{-1}}$ (better than 1%).[2] This level of precision is new for the field of observational cosmology, where until as recently as a couple of decades ago, a factor-of-two uncertainty had persisted for several decades. In a sense, this new level of precision has led to high expectations for other types of cosmological measurements. Yet, obtaining equally high precision observations of the local measurements of H_0 remains a formidable challenge. At face value, the inconsistency between the local value of the Hubble constant and the cosmologically modeled value could be interpreted as an inadequacy in the theory, thereby begging the questions: is cosmology in a crisis? And is our current model of the universe now in need of new physics?

While acoustic oscillations of the ionized plasma in the early universe are well understood and based on linear physics, it is important to keep in mind that the astrophysics of stellar distance indicators is less predictive from first principles; and the requirement of accurate *absolute* calibrations of the local distance scale at a comparable (1%) level, with the identification and elimination of systematic effects for evolving stars (which may be located in dusty, crowded regions) are tall orders. Given the current challenges in obtaining percent level accuracy in the local distance measurements, it may be premature to be claiming either confirmation, or the refutation, of the need for physics beyond the standard model [16]. These remaining challenges underscore the need for a definitive measure of H_0 locally, which in turn demands a complete and independently confirmed assessment of its total (statistical and systematic) uncertainties [17].

[1] It is now appreciated that Lemaitre [4] had earlier found a mathematical solution for an expanding universe, recognizing that it provided a natural explanation for the observed recession velocities of galaxies, but these results were published in French in the Annals of the Scientific Society of Brussels, and at that time were not widely accessible.

[2] For a discussion of possible systematics in the CMB analysis see [15] and references therein.

JCAP11(2023)050

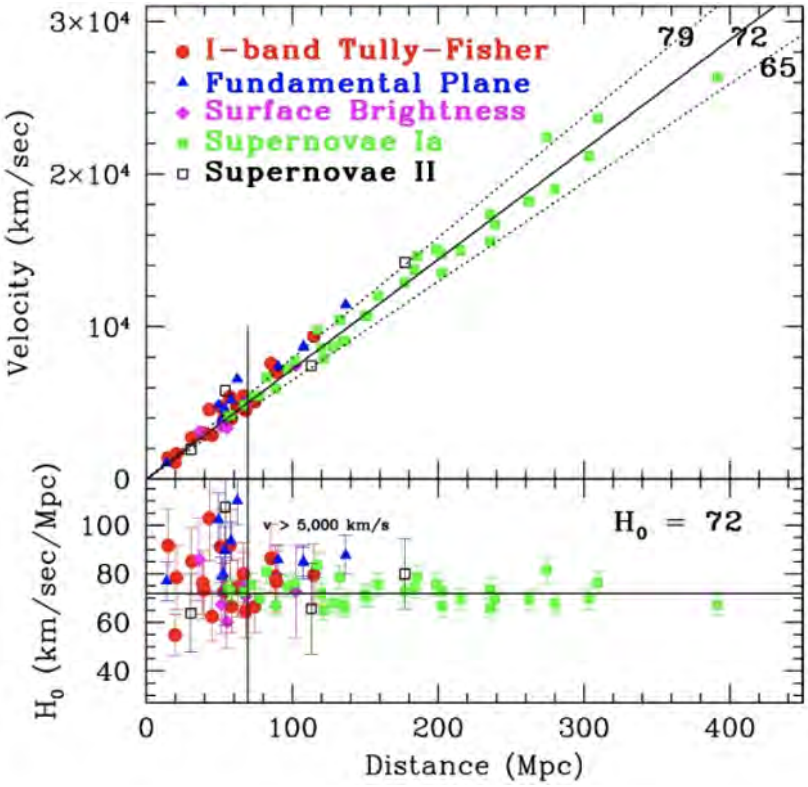

Figure 1. The Key Project Hubble Diagram: distances in Mpc vs flow-corrected velocities in km/s. Secondary distance indicators used in this diagram are color-coded and identified in the legend at the top left of the figure. Residuals from a fit of $H_0 = 72 \pm 7$ km/s/Mpc are shown in the lower panel. SNe extend out the farthest of the secondary methods and have the lowest dispersion. The other methods have a greater scatter owing to peculiar velocities and bulk flows. The vertical line denotes a velocity of 5000 km/s. Reproduced from [5].

JCAP11(2023)050

Ascertaining whether additional physics is required beyond the standard ΛCDM model, although a challenge, is a surmountable observational issue. It will require the establishment of several independent calibrations of the local distance scale, each with high precision, to provide robust constraints on the overall systematics.

In this review, we briefly summarize historical efforts in the direct, local (astrophysical) measurements of H_0, present highlights from the past two decades in refining the measurements, discuss the substantial progress in overcoming systematic uncertainties, and note where we can expect most progress in the coming years, including very exciting new results from *JWST*. In an appendix, we compare and contrast the strengths and weaknesses of the most promising methods in use today for measuring distances in the local universe. The prospects are good for a resolution to the *local* (distance scale) version of the H_0 tension. The past 20 years have been referred to as the era of 'precision cosmology'. We must now ensure that we have convincingly entered the era of 'accurate cosmology'.

2 The landscape at the turn of the century: the Hubble Key Project

The launch of HST in 1990 provided the opportunity to undertake a major program to calibrate the extragalactic distance scale. The HST Key Project was designed to measure the Hubble constant to a total (statistical plus systematic) uncertainty of ±10% [5]. Given that the dominant sources of error were clearly systematic in nature, the approach taken in the Key Project was to measure H_0 by intercomparing several different methods, each having minimally overlapping systematics. The goal was to extend and apply the Cepheid distance scale beyond what could be achieved from the ground, and then to assess and to quantify the overall systematic errors in the measurement of H_0. Observations were obtained in the V band (F555W; 12 epochs within a 60-day window + 1 additional epoch a year later, to avoid aliasing effects) and the I band (F814W; 4 epochs). The roll angle of the telescope was held fixed for all of the observations to maximize overlap of the different epochs and to facilitate the photometric measurements. Data were taken with a power-law spacing to minimize aliasing effects [18]. In addition, a test for the metallicity dependence of the Cepheid PL relation was undertaken.

Cepheids are supergiant stars, but they are still not sufficiently bright that they can be used to determined distances far enough away to sample the unperturbed cosmic Hubble flow. Large-scale flows generated by major clusters, filaments and voids induce so-called "peculiar velocities" on one another and on individual field galaxies. This ubiquitous source of noise in the velocity field must either be modelled out, averaged over large samples, or diminished in its relative impact by going out to distances where the Hubble flow is dominant. To make that leap secondary distance indicators of higher luminosity, (but often of lower precision and accuracy), were invoked. The secondary distance indicators specifically targeted by the Key Project for zero-point calibration by the Cepheids were the Tully-Fisher relation, the Surface Brightness Fluctuation method and the Fundamental Plane of galaxies, as well as two types of extremely bright explosive events, Type I and Type II supernovae.

None of the secondary distance indicators have first-principles physics backing them up; they are largely empirical distances indicators. Type Ia supernovae have most recently become the secondary indicator of choice because of 1) their brightness, which allows them to probe cosmological distances, 2) their standardizable maximum-light luminosities and 3) their low scatter in the Hubble diagram. At lower redshifts these candles are found to have absolute magnitudes with a dispersion of less than 5–6 percent per event [19]. Establishing the absolute zero point of Type Ia supernovae quickly became the *de facto* standard means of deriving the local value of the expansion rate of the universe, with Cepheids providing the zero point calibration.

The final result from the HST Key Project, $H_0 = 72 \pm 3$ (stat) $\pm$ 7 (sys) $\mathrm{km\,s^{-1}\,Mpc^{-1}}$, was based on Cepheid distances to 31 galaxies, 18 of which were newly measured as part of the Key Project. The largest contribution to the systematic uncertainty (5%), at that time, was that of the distance to the calibrating galaxy, the Large Magellanic Cloud (LMC), to which the distance had been measured using a wide variety of independent techniques.

In what follows, we discuss in detail the two currently highest-precision methods for measuring distances to nearby galaxies, and for providing a tie-in to SNe Ia: Cepheids and the Tip of the Red Giant Branch (TRGB) method. For nearby galaxies, these two methods

currently have the lowest measured scatter, their distances can be compared *galaxy by galaxy within the same galaxies*, and they can be applied individually to samples of dozens of galaxies, in sharp contrast to other techniques at the moment.

We pay particular attention to systematic uncertainties, the essential issue in the measurement of galaxy distances, the determination of H_0, and for settling the question of whether there is additional physics beyond ΛCDM.

3 Progress since the Key Project: the Cepheid distance scale: 2001–2023

Cepheids have held the place of being the gold standard for the measurement of extragalactic distances ever since Edwin Hubble's discovery of the expansion. A recent review of Cepheids as distance indicators is given by Freedman & Madore [20]. For more details on the nature of Cepheid variables themselves, the reader is also referred to some earlier reviews [21–24].

Following on the Key Project, Macri et al. [25] obtained H band (F160W) observations of a subset of the Key Project galaxies using NICMOS on HST. Their findings supported the assumption of universality for the extinction law for Cepheids: the VI photometry used in the Key Project Cepheid distance scale agreed with the augmented VIH distances employing the additional near-infrared observations. This result suggested that there is no (extinction law) advantage in going to the extra effort to move the Cepheid calibration and its application into the IR. The study additionally showed that the lower spatial resolution in the H band imaging data led to more serious crowding effects than in the optical, an issue of even more concern as the sample of galaxies is augmented to include galaxies farther away.

3.1 Chicago Carnegie Hubble Program (CCHP)

The goal of the Chicago Carnegie Hubble Program (CCHP) is to increase the accuracy of measurements of H_0. Initially begun 15 years ago (as the Carnegie Hubble Program), the program was designed as a follow-up to the HST Key Project, taking advantage of the mid-infrared capabilities of the Infrared Array Camera (*IRAC*) on *Spitzer*, and was undertaken in anticipation of the launches of *Gaia* and *JWST* [7]. It followed up on HST *NICMOS* observations made in the F160W bandpass [25] for Cepheids in 12 nearby galaxies, and the detailed JHK (complete lightcurve coverage) near-infrared, ground-based study of 92 Cepheids in the LMC [26]. Over time, the program was expanded to include not only Cepheids, but also TRGB [27, 28] and J-region Asymptotic Giant Branch (*JAGB*) stars [29–31], each of these being independent means of calibrating Type Ia supernovae (SNe Ia) and thereby, H_0. The current focus of the CCHP is directed at exploiting the superb infrared sensitivity and high spatial resolution of the *JWST* to improve the accuracy and precision of all three of these methods.

3.2 Supernova Ho for the Equation of State (SHoES)

The SHoES program [9, 13] has the goal of using *HST/ACS* and *HST/WFC3* to extend and improve the Cepheid calibration of SNe Ia for a measurement of H_0. Most recently, they have obtained NIR observations of Cepheids in 42 SN Ia host galaxies (figure 2) with the aim of reducing the systematic uncertainties due to reddening and metallicity. Reddening corrections

JCAP11(2023)050

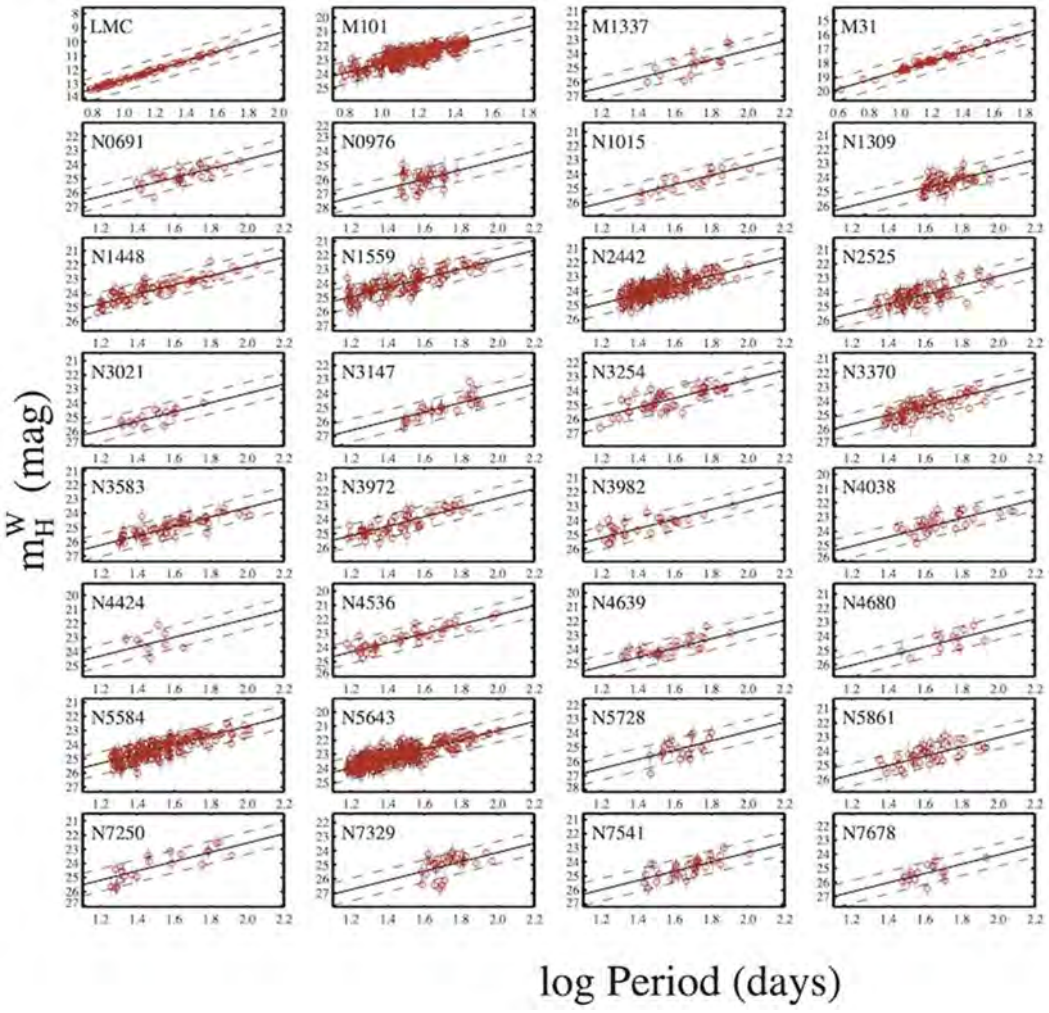

Figure 2. A sampling of reddening-free near-IR Wesenheit magnitude PL relations. Note the four-times larger scatter seen in virtually all of the SHoES galaxies compared to the fiducial scatter seen in the LMC and M31 (top row). Reproduced from [9]. The Author(s). CC BY 4.0.

are obtained using a small number of (2 to 3) single-phase observations in the F814W and F555W bands from *HST/ACS*. The distances are based primarily on ∼6 low-signal-to-noise observations taken in the F160W (H) band. The resulting scatter in the F160W period-luminosity relations is typically of order ±0.4–0.5 mag, which is about a factor of four times greater than the intrinsic dispersion observed in the uncrowded sample of Cepheids in the LMC, for instance. The zero-point calibration is set by Early Data Release 3 (EDR3) geometric parallaxes, masers in the galaxy NGC 4258, and detached eclipsing binaries in the LMC. Their most recent result quotes a 1% uncertainty with $H_0 = 73.04 \pm 1.04\,\mathrm{km\,s^{-1}\,Mpc^{-1}}$, based on their sample of 42 galaxies with distances in the range from 7 out to 80 Mpc.

4 Tip of the Red Giant Branch (TRGB) distance scale: 1993–2023

The TRGB provides one of the most precise and accurate means of measuring distances in the local universe. Observed color-magnitude diagrams of the Population II stars in halos

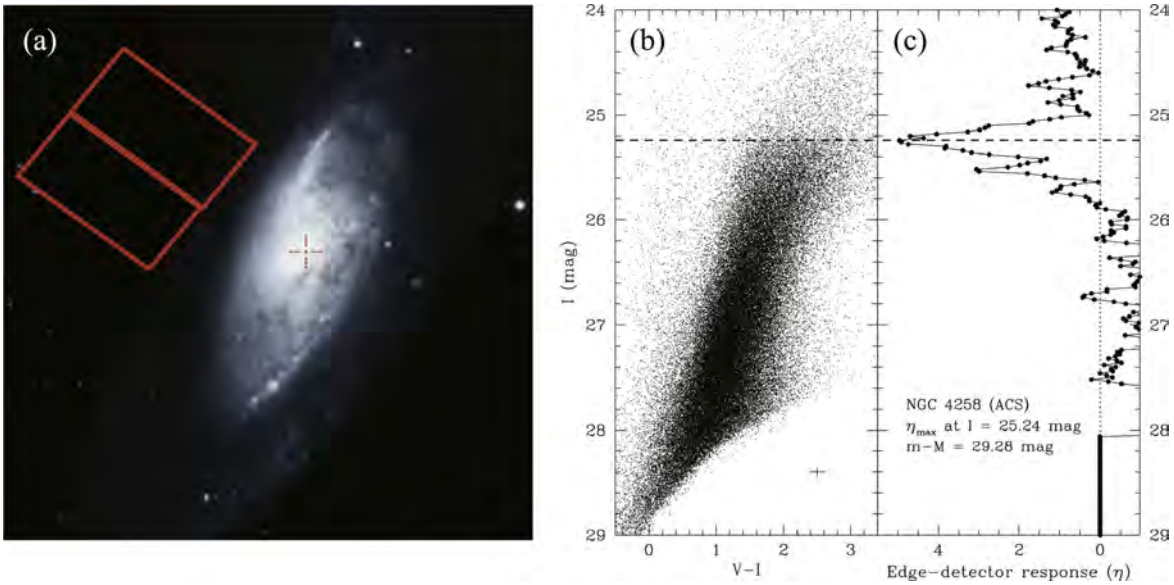

Figure 3. Left Panel — An example of a halo field chosen to be along the minor axis of the galaxy NGC 4258. Right Panel — The I-band vs (V-I) color-magnitude diagram for the RGB stars detected in the halo of NGC 4258. To the far right is the Sobel filter edge-detector response function applied to the RGB luminosity function. The peak in the edge detector indicates the discontinuity defining the TRGB. Reproduced from [48]. © 2008. The American Astronomical Society.

of nearby galaxies reveal a sharp discontinuity in the red giant branch (RGB) luminosity function at a well-determined magnitude (see figure 3). This feature is easily identified and corresponds to the core helium-flash luminosity at the end phase of RGB evolution for low-mass stars. As a result, the TRGB provides a superb standard candle in the I band [27, 32–36], and it is a standardizable candle in the near infrared [37–40]. The method is described in more detail in a number of reviews [23, 41, 42].

In brief, the underlying theory for why the TRGB is an excellent standard candle is well-developed [43–47]. For low-mass stars with masses $M \lesssim 2M_{\odot}$, their evolution ascending the red giant branch consists of a shell that is burning hydrogen immediately above a degenerate helium core. The mass of the helium core increases with freshly formed helium from the shell burning, until the core mass reaches a threshold value of about 0.5 $M_{\odot}$ independent of the initial mass of the star. At this stage the core will have reached a temperature of about 10^8 degrees, at which point the triple-alpha process (helium burning) can commence. Because the core is degenerate and cannot expand, a thermonuclear runaway ensues, injecting energy that overcomes the core degeneracy, and changing the equation of state. The star then rapidly evolves off the red giant branch to the (lower-luminosity) horizontal branch or the red clump, thereafter undergoing sustained core helium burning.

The TRGB method has been used widely for the determination of distances to galaxies of various types in the local universe. The application of the TRGB method far exceeds the number of measurements of Cepheid distances.[3] The reason is practical: Cepheids are variable

[3]Approximately 1,000 TRGB distances to about 300 galaxies are compiled in NED; less than 70 galaxies have Cepheid distances to date.

JCAP11(2023)050

stars requiring observations at many epochs to determine periods, amplitudes and light curves for the construction of time-averaged period-luminosity relations. In contrast, TRGB stars are non-variable and have constant I-band magnitudes as a function of color and metallicity, requiring only a single-epoch observation. In addition, TRGB stars can be observed in galaxies of all morphological types, whereas Cepheids are present only in late-type galaxies.

4.1 Chicago Carnegie Hubble Program (CCHP) and the TRGB

One of the primary goals of the Chicago Carnegie Hubble Program (CCHP) is to pursue an alternative route to the calibration of SNe Ia and thereby provide an independent determination of H_0 via measurements of the TRGB in nearby galaxies. This method has a precision equal to or better than the Cepheid Leavitt law, and its current accuracy is also comparable. The calibration of the zero point of the I-band TRGB method and its application to the extragalactic distance scale has recently been reviewed by Freedman [28].

Freedman et al. [27] presented a determination of H_0 based on TRGB distances to 15 galaxies that were hosts to 18 Type Ia supernovae (SNe Ia). The *HST/ACS* fields were selected to target the halos of the galaxies where the effects of dust are minimal, and, at the same time, to specifically avoid contamination by younger and brighter disk asymptotic giant branch (AGB) stars. This calibration was then applied to a sample of 99 significantly more distant SNe Ia that were observed as part of the Carnegie Supernova Project (CSP) [49]. The calibration has been updated [10, 28], and is currently based on our independent calibrations of the TRGB absolute magnitude that are internally self consistent at the 1% level. The method yields a value of $H_0 = 69.8 \pm 0.6$ (stat) $\pm$ 1.6 (sys) $\mathrm{km\,s^{-1}\,Mpc^{-1}}$. This value differs only at the 1.2σ level from the most recent Planck Collaboration [14] value of H_0. It is smaller than previous estimates of the Cepheid calibration of SNe Ia [7, 9] but still agrees well, at better than the 2σ level. Alternatively, adopting the SNe Ia catalog from the *SHoES* collaboration [50] results in little change with $H_0 = 70.4 \pm 1.4 \pm 1.6\,\mathrm{km\,s^{-1}\,Mpc^{-1}}$ [27].

Comparisons of the CCHP TRGB distances with those in the Extragalactic Distance Database (EDD) were undertaken by [51] and [52]. These comparisons provide an important external check of the TRGB method since different approaches to the analysis were taken, and carried out completely independently by separate research groups. For example EDD used DOLPHOT and applied a maximum likelihood fitting method whereas the CCHP used DAOPHOT and an edge-detection (Sobel filter) algorithm. Adopting a consistent NGC 4258 calibration, the difference is only 0.001 $\pm$0.048 mag [51] (see figure 4). A remaining difference is the absolute calibration of the TRGB at the 0.06 mag level (see [28] and [52], line 1, table 4). This difference results from the choice to calibrate either in the outer halo (CCHP) or the disk of NGC 4258 (EDD). As discussed further below, the outer halo provides a less complex (dust-free and uncrowded) environment, offering better precision and accuracy in the measurement.

4.2 Remaining challenges in measuring the TRGB

The measurement of precise TRGB distances necessitates locating a clear edge to the red giant branch luminosity function. In practice, these measurements can be complicated by the photometric measurement uncertainties, the sample size (numbers of stars defining the

JCAP11(2023)050

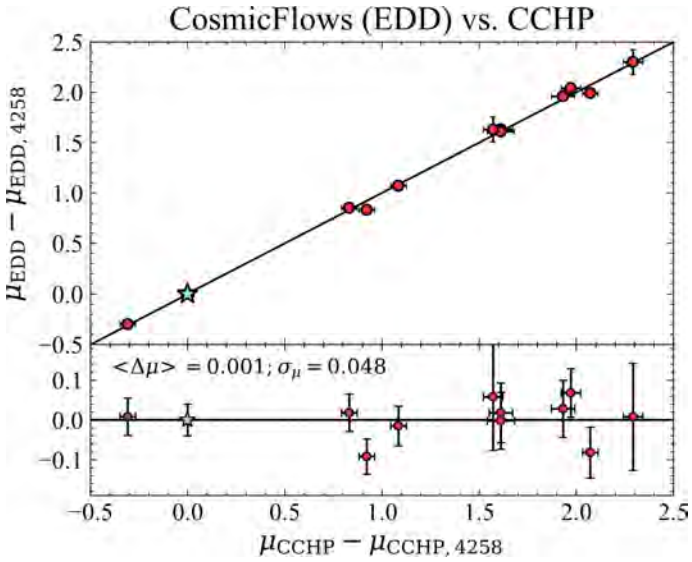

Figure 4. A comparison of TRGB distances from the EDD [52] and the CCHP [27, 36, 51, 53]. The distances are calibrated relative to NGC 4258 (blue star). A line of unit slope is shown in the top panel. In the bottom panel, the median offset value is shown (dashed line), as well as at zero offset (solid line). These two independent analyses show excellent agreement.

tip), and contamination from a brighter population of AGB stars; factors which present a challenge, especially for the current level of precision and accuracy demanded for testing current cosmology. These issues have recently been addressed through a series of simulations by Madore & Freedman [42], quantifying the uncertainties in the TRGB method. The conclusion from these simulations is that for *precision and accuracy*, the method should be applied in the outer halos of galaxies where the effects of dust extinction and self crowding by red giant branch stars are minimal. Measurements of the TRGB in the higher surface brightness disks of galaxies confront the complexity of dust, gas, stars of mixed ages, colors and crowding, which act to degrade the TRGB detection (smearing out the edge and/or introducing multiple peaks).

A different approach has been adopted by [54] (and references therein) who have undertaken to provide an 'optimized unsupervised algorithm' (called CATS) to measure TRGB distances and determine H_0, extending measurements of the TRGB into the disks of galaxies. They find a value of $H_0 = 73.22 \pm 2.06\,\mathrm{km\,s^{-1}\,Mpc^{-1}}$, apparently in better agreement with the Cepheid calibration. This method uses a 'contrast ratio R', defined by the number of stars above and below the tip. Unfortunately, this unsupervised method in its current form, is susceptible to mistaking the asymptotic giant branch (AGB) for the RGB (e.g., NGC 4038), a problem that is known and has been addressed by many authors previously in the literature [55–57]. For NGC 4038 and NGC 4536, the TRGB distances that their unsupervised algorithm gives the highest weight to (having higher contrast values) are significantly closer than the published *SHoES* Cepheid distance measurements [9] by 0.7 and 0.6 mag, that is 30% and 40% offsets in distance, respectively, and ultimately contribute a higher H_0 value than other measurements based on the TRGB [10–13]. These results also differ appreciably from the excellent agreement between the published Cepheid distances in Riess et al. [9] and TRGB

JCAP11(2023)050

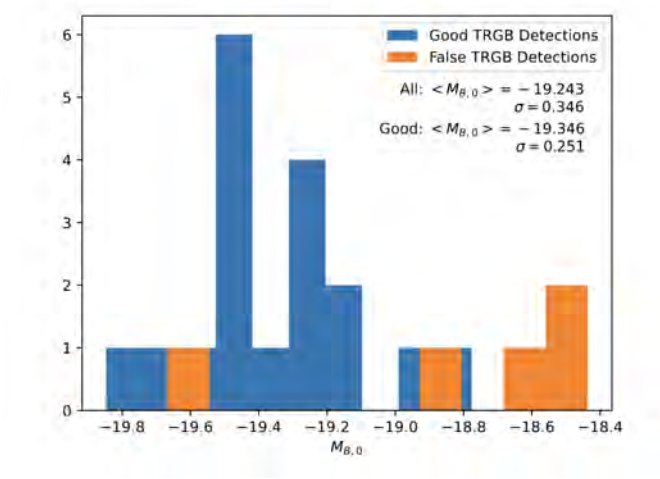

Figure 5. Histogram of the peak SNe Ia magnitudes from tables 1 and 2 and equation 3 of Scolnic et al. [54] (Hoyt, private comm.) The cases where the AGB has been mistakenly identified for the RGB are shown in orange. The dispersion in the SNe Ia peak magnitudes is erroneously increased as a result of these anomalously fainter magnitudes, biasing the result and leading to a higher value of H_0.

distances in Freedman et al. [27], which in the mean, agree to 0.007 mag. Additionally, in adopting the unsupervised TRGB distances, the *rms* dispersion in the SNe Ia peak magnitude for the TRGB SNe Ia host galaxies increases from ±0.12 mag [27] to ±0.346 mag (see figure 5, Hoyt private communication). The scatter in the SNe Ia peak magnitudes increases to a level that is a more than a factor of three greater than that seen in the distant SNe Ia, ±0.10 [58].

In future, the accuracy of the TRGB distance scale will continue to improve with additional observations in the outer halos of galaxies; i.e., programs designed specifically to avoid (unnecessary) additional complexities (and potential systematics) introduced by working in crowded regions of star formation, dust, etc.

5 Anchors to the distance scale

At present the overall accuracy in the determination of H_0 is limited by the small number of galaxies that 'anchor' the Cepheid and TRGB distance scales; that is, galaxies for which there are geometric distances, acting as the first stepping stones out to the more distant galaxies. In the case of the Cepheid distance scale, there are only three such anchors: the Milky Way, the Large Magellanic Cloud (LMC) and the maser galaxy NGC 4258. In the case of the TRGB, there is one additional anchor, the Small Magellanic Cloud (SMC). JAGB stars also have the Milky Way, LMC, SMC and NGC 4258 as anchors.

5.1 Large Magellanic Cloud (LMC)

At the conclusion of the Key Project, the largest component of the systematic error budget was the contribution from the adopted uncertainty to the distance of the LMC. A distance modulus to the LMC of 18.5 mag was adopted, with a very conservative uncertainty of ± 0.1 magnitudes, reflecting the wide range of published distance moduli at the time (18.1 to 18.7 mag) [5].

JCAP11(2023)050

The distance modulus to the LMC has been improved significantly since the time of the Key Project, based on measurements of 20 detached eclipsing binary (DEB) stars in the LMC [59]. This method gives a distance modulus of 18.477 ± 0.004 (stat) ± 0.026 (sys), corresponding to a distance uncertainty of only 1.2%. The DEB value is in exact agreement with measurements of the Cepheid Leavitt law based on 3.6 μm mid-infrared measurements from the Spitzer Space Telescope [60, 61]. Furthermore this value is only 0.023 mag different from the Key Project value, meaning that the LMC zero-point calibration adopted at that juncture has withstood the test of time, at a ∼1% level of accuracy.

5.2 Milky Way parallaxes: Hipparcos, HST and Gaia

There have also been enormous gains in the measurement of parallaxes to Cepheids in the Milky Way in the past 20 years, from *Hipparcos* [62] to HST and its Fine Guidance Sensor [63–65] (which provided the calibration for the Spitzer Cepheid PL relation [7]), culminating most recently with measurements from *Gaia* [66, 67]. The *Gaia* measurements are revolutionizing studies of the Milky Way; for example, see [68].

The *Gaia* Early Data Release 3 (EDR3) database [69] contains parallaxes, proper motions, positions and photometry for 1.8 billion sources brighter than G = 21 mag [67]. At the end of its mission, *Gaia* is expected to provide astrometry reaching tens of microarcsecond accuracy. For Milky Way Cepheids, TRGB stars and other distance indicators, this level of accuracy will ultimately set the absolute calibration to an accuracy of <1%, an accuracy critical for helping to resolve the H_0 tension. However, this challenging high accuracy has not yet been achieved owing to a zero-point offset [70] resulting from the fact that the basic angle between the two *Gaia* telescopes is varying. There is a variance in the parallaxes (the systematic uncertainty measured relative to the background-quasar reference frame, defined by 550,000 quasars in the International Celestial Reference System) and a zero-point offset of –17 μas (in the sense that the *Gaia* parallaxes are too small). Unfortunately this offset results in a degeneracy with the absolute parallax, and is limiting the ultimate accuracy required to reach the 1% target. In addition, these variations lead to zero-point corrections that are a function of the magnitude, color, and position of the star on the sky [71, 72]. The *Gaia* Collaboration has emphasized [73, 74] that not only is there a significant variance in these measured offsets over the sky, but the EDR3 uncertainties in the parallaxes for different objects are correlated as a function of their angular separations [66, 67].

Many efforts have been made to improve the parallax uncertainties from *Gaia* DR3 data [74–77]. Future releases from *Gaia* DR4 and DR5 will continue to improve the parallax measurements and their uncertainties, and establish a definitive Milky Way calibration.

5.3 NGC 4258

The nearby spiral galaxy NGC 4258, at a distance of 7.6 Mpc, provides an additional anchor or zero-point calibration for the local distance scale. This galaxy is host to a sample of H_2O megamasers within an accretion disk that is rotating about a supermassive black hole, from which a geometric distance to the galaxy has been measured [78, 79]. (For more details on the method, see section 8.2.) The geometric distance modulus measured most recently to NGC 4258 is μ_o = 29.397 ± 0.033 mag [79], a 1.5% measurement.

JCAP11(2023)050

As a consistency check, the distance to NGC 4258 can be determined based on HST measurements of the TRGB in its outer halo, calibrated by the LMC [80]. Adopting the measured apparent TRGB magnitude of $m_{o\,F814W}^{N4258} = 25.347 \pm 0.014 \pm 0.005$ [36], results in a distance modulus of $\mu_o = 29.392 \pm 0.018 \pm 0.032$ mag that agrees with the maser distance modulus of 29.397 ± 0.033 mag at a level of better than 1% ($<0.2\sigma$).

The Cepheid calibration, however, does not yield as good agreement with that of the maser distance, and ultimately depends on the sensitivity of Cepheid luminosities to metallicity. For example, a calibration of the Cepheid distance to NGC 4258 based on the LMC differs from the maser distance by 2.0–3.5σ, adopting different published slopes for the metallicity correction [81]. However, since the Milky Way and NGC 4258 metallicities are very similar, a calibration of NGC 4258 based on the Milky Way should be independent of a metallicity effect. Yet, if the Milky Way is adopted as the anchor galaxy to determine the Cepheid distance to NGC 4258, a distance modulus of 29.242 ± 0.052 is obtained, which differs from the maser distance by 7% at a 2σ level of significance. Careful scrutiny of the distances to anchor galaxies remain important in the context of assuring that a 1% H_0 value is in hand.

6 Type Ia supernovae

The numbers of well-observed SNe Ia useful for measuring H_0 has continued to grow with time [82]. These include the nearby SNe Ia out to distances of ∼30–40 Mpc that can be calibrated using HST distances from the TRGB or Cepheids. If systematic effects due to crowding can be established to be small (but see section 9.1 below), perhaps the calibration can be reliably extended to $\gtrsim$50 Mpc. The *SHoES* collaboration now has 42 galaxies for which Cepheids have been discovered, out to a distance of 80 Mpc. The nearby SNe Ia that can be observed with HST that occur in galaxies for which the TRGB or Cepheids can be measured typically occur only about once per year [9].

We discuss below two programs that currently calibrate the Cepheid and TRGB distance scales: the Carnegie Supernova Project (CSP) and Pantheon+.

6.1 Carnegie Supernova Project (CSP)

The goal of the CSP was to provide a homogeneous, intensive, high-cadence, multi-wavelength ($uBVgriYJH$) follow-up of nearby SNe Ia and SN II [83]. Not a survey program, the idea was to obtain a consistent data set with careful attention to photometric precision and systematics, critical for applications to cosmology, as well as for studying the physical properties of the supernovae themselves.[4] The program utilized a fixed set of instruments, photometric standard stars, and instrumental reduction procedures, catching most of the supernovae well before maximum, and with high signal to noise, avoiding the challenges otherwise faced in minimizing systematic differences between multiple data sets/instruments/etc. [49]. Optical spectra were also obtained with high cadence [84]. The bulk of the observations were carried out at Las Campanas Observatory using the 1-m Swope and 2.5-m du Pont telescopes. The first part of the CSP (CSP-I) was carried out from 2004–2009. A second phase of the CSP (CSP-II) was carried out from 2011–2015, and was optimized for the near-infrared [85, 86].

[4]The CSP data are available at http://csp.obs.carnegiescience.edu/data.

JCAP11(2023)050

The reduction of the CSP light-curve photometry was undertaken using an analysis package called SNooPy [58]. The Hubble diagram for the CSP-I SNe Ia sample, calibrated by Cepheid distances from [87] was presented in [58]. These authors found a value of $H_0 = 73.2 \pm 2.3\,\mathrm{km\,s^{-1}\,Mpc^{-1}}$ based on H-band data; and a value of $H_0 = 72.7 \pm 2.1\,\mathrm{km\,s^{-1}\,Mpc^{-1}}$ using B-band data. A TRGB calibration of the CSP-I sample was given by [27] and updated in [10, 28]. As discussed in section 4.1 above, the TRGB calibration gives a slightly lower value of $H_0 = 69.8 \pm 0.6$ (stat) $\pm$ 1.6 (sys) $\mathrm{km\,s^{-1}\,Mpc^{-1}}$.

Recently [88] have used the SNe Ia data from the CSP-I and II (an increase by a factor of three in the numbers of SNe Ia over CSP-I alone) to calibrate the Cepheid distance scale, as well as the TRGB (and Surface Brightness Fluctuations, a secondary distance indicator). Using B-band light-curve fits, they find $H_0 = 73.38 \pm 0.73\,\mathrm{km\,s^{-1}\,Mpc^{-1}}$ based on a calibration of Cepheids. For the TRGB calibration, they find $H_0 = 69.88 \pm 0.76\,\mathrm{km\,s^{-1}\,Mpc^{-1}}$, both in good agreement with previously published Cepheid and TRGB studies.

6.2 Pantheon+

The Pantheon+ analysis [89] currently consists of 1550 individual SNe Ia, superseding earlier Pantheon [90] and Joint Light-Curve [91] analyses. The analysis knits together and standardizes the B-band photometry from 18 individual surveys obtained with a wide variety of telescopes and instruments.[5] The sample includes SNe Ia in the redshift range $0 < z < 2.3$; the subset used for constraining H_0 are those for which $0.023 < z < 0.15$.

The *SHoES* Cepheid calibration of the Pantheon+ SNe Ia sample from [89] results in a value of $H_0 = 73.04 \pm 1.04\,\mathrm{km\,s^{-1}\,Mpc^{-1}}$ for the 277 SNe Ia with $0.023 < z < 0.15$, as noted previously in section 3.2.

Ultimately, it is expected that the SNe Ia samples will continue to grow as future large-scale (and homogeneous) surveys like the Legacy Survey of Space and Time (LSST) [92] and the Nancy Grace Roman Space Telescope [93] become available.

7 J-Region Asymptotic Giant Branch (JAGB) distance scale: 2000–2023

The JAGB method is emerging as one of the most promising methods for measuring the distances to galaxies in the local universe. JAGB stars were first identified as a distinct class of objects in the LMC [94, 95], demonstrated to be very high precision distance indicators, and then successfully used to map out the back-to-front geometry of the LMC. Two decades later the method was applied in an extragalactic distance scale context [29, 30, 96]. Together, these studies have demonstrated that there is a well-defined class of carbon stars with a nearly constant luminosity in the near-infrared; i.e., an excellent standard candle for distance measurements. These (thermally-pulsating AGB) stars have a low intrinsic dispersion, specifically in the near-infrared J band, of only $\pm$0.2 mag [94], and they can be identified on the basis of their near-infrared colors alone, being distinguished from bluer O-rich AGB stars, as well as being segregated from redder, extreme carbon stars (see figure 6).

Freedman & Madore (2020) measured JAGB carbon-star distances to a sample of 14 galaxies out to 27 Mpc, calibrated using the LMC and the SMC, and compared them to

[5] The Pantheon+ catalog is available at https://github.com/PantheonPlusSH0ES/DataRelease.

JCAP11(2023)050

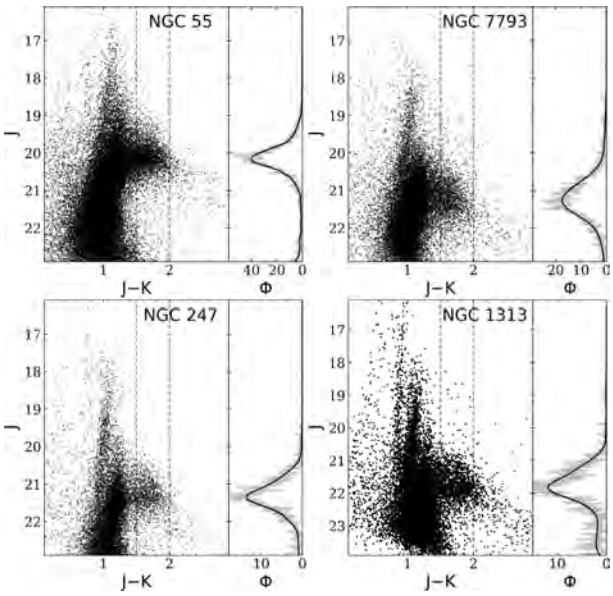

Figure 6. Ground-based (Magellan/FourStar) near-infrared CMDs of four nearby galaxies observed by Lee et al. (in preparation), illustrating the well defined, single peaked J-band luminosity functions characteristic of the JAGB population in the color range 1.5 < (J-K) < 2.0.

previously published distances using the TRGB. They found that the distance moduli agreed extremely well (at the 1% level), with a (combined) scatter amounting to only ±4%. The good agreement with the TRGB distances suggests that the effects of metallicity for this well-defined color-range of carbon stars are small. A number of additional extensive tests of this method have recently been carried out by Lee and collaborators [31, 97, 98] as well as Zgirski et al. [99] in several nearby galaxies, confirming the excellent agreement with distances measured with the TRGB and Cepheid distance scales, and again indicating that metallicity and star formation effects are small (see figure 7).

Recent modeling of AGB star evolution has been carried out by many authors [100–102]. Significant challenges remain in the detailed modeling (e.g., treatment of convection, overshoot, winds and mass loss), but the broad outlines are well-characterized. A carbon star is defined such that the atmosphere contains more carbon than oxygen; i.e., a ratio of C/O >1. The path to becoming a carbon star occurs during the thermally pulsing evolutionary phase for AGB stars. As a result, carbon can be brought to the surface, particularly during the third and later (generally deeper) dredge-up phases [103–105]. For stars with solar metallicity, recent studies conclude that the initial mass for carbon-star formation is between 1.5 and 3.0 to 4.0 $M_\odot$ [106], with a similar range for stars with Z = 0.008 [102].

The reason for the well-constrained luminosity of carbon stars is two-fold: (1) younger, more massive (hotter) AGB stars burn their carbon at the bottom of the convective envelope before it can reach the surface of the star [107], whereas (2) for the oldest, less massive AGB stars, there is no third, deep dredge-up phase. Thus, carbon stars are formed only in the intermediate mass range where carbon-rich material can both be dredged up and survives so that it can be mixed into the outer envelope.

JCAP11(2023)050

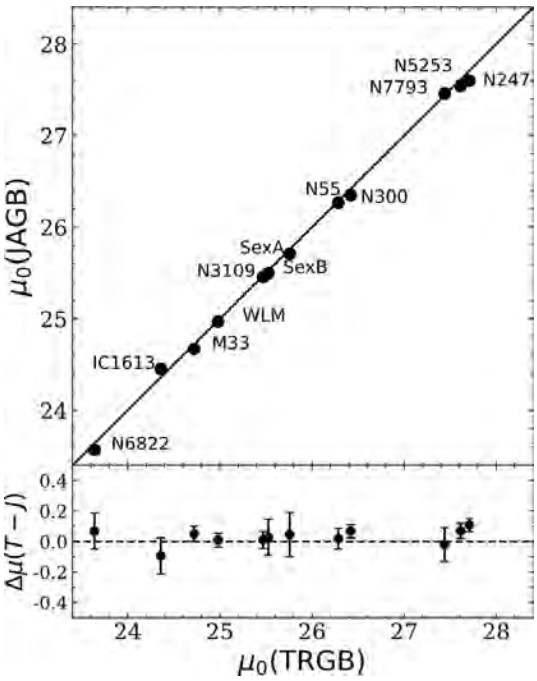

Figure 7. Comparison of ground-based JAGB and TRGB distance moduli to a dozen nearby galaxies (Lee et al. in preparation). The lower panel shows the magnified differences between the moduli which have a combined scatter of only ±0.06 mag. For this sample of galaxies this scatter puts upper limits (of a few percent) on the impact of metallicity differences, differential internal reddening and potential star formation history differences between these galaxies.

In summary, the JAGB method offers a number of advantages for distance measurement, as previously enumerated [30]. (1) They are easily identified by their colors and magnitudes in the infrared. (2) They have a low intrinsic dispersion in the J band of only ±0.2 mag. (3) They are about one magnitude brighter than those defining the TRGB. (4) They are found in all galaxies that have intermediate-age populations, and the JAGB method is, therefore, applicable to a wide range of galaxy types. (5) Near-infrared observations offer the advantage of reduced intrinsic variability and reduced reddening. (6) No multi-epoch observations are required to determine periods as, for example, is the case for Cepheid and Mira variables; observations of JAGB stars in two infrared bands, at a single epoch, are all that is needed.

With further development, testing and application the JAGB method has the potential to provide an independent calibration of Type Ia supernovae (SNe Ia), especially with *JWST*. JAGB stars are brighter than the TRGB and thus can be detected at greater distances, allowing greater numbers of calibrating galaxies for the determination of H_0. As is the case for the TRGB and Cepheids, JAGB stars are amenable to theoretical understanding and further improved empirical calibration. Early tests show little dependence, if any, of the JAGB magnitude with metallicity of the parent galaxy (see Lee et al. [98] and figure 9), and therefore suggest that the JAGB method has considerable promise for providing high-precision distances to galaxies in the local universe that are largely independent of distances derived from the Leavitt Law and/or the TRGB method.

JCAP11(2023)050

8 Other methods

8.1 Surface Brightness Fluctuations (SBF)

For most distance indicators crowding of individual stars by the surrounding population of stars is a major source of systematic uncertainty; a systematic that increases in its effects as the targets being measured are found at increasing distances. Thirty-five years ago Tonry & Schneider [108] introduced a novel technique, called the Surface-Brightness Fluctuation (SBF) method that takes crowding (a systematic effect that depends on distance) and turns a quantitative measure of the crowding into a means of measuring distances. The method has recently been extensively reviewed in [109].

The SBF method applies best to elliptical galaxies, and with caution, to the bulges of bright, early-type spiral galaxies, where the effects of dust and recent star formation can be mostly avoided. At a given surface brightness (which is by definition independent of distance) the degree of crowding of any pre-specified population of stars will increase/degrade with distance as the mean separation of those same stars also decreases inversely with distance. A measure of the observed granularity in the image, which is used to determine a distance, is found in the power spectrum of the targeted field of view.

Recent applications of the SBF method have led to values of $H_0 = 73.3 \pm 0.7$ (stat) $\pm$ 2.4 (sys) [110], $H_0 = 70.50 \pm 2.37$ (stat) $\pm$ 3.38 (sys) [111] and $H_0 = 74.6 \pm 0.9$ (stat) $\pm$ 2.7 (sys) $\mathrm{km\,s^{-1}\,Mpc^{-1}}$ [112], respectively. The most important error terms [109] are (i) sky background subtraction [0.02 mag], (ii) characterization of the point spread function [0.03 mag], (iii) details of the power spectrum fitting [0.02 mag], (iv) residual variance in the power spectrum, due to globular clusters and background galaxies too faint to be detected and masked directly [0.05 mag], and (v) extinction. Values in square brackets are the errors due to these terms as estimated by [109] section 1.4.1.

Finally, it should be noted that the SBF method is a secondary distance indicator (as are other notable examples, including Type Ia supernovae and the Tully-Fisher relation) given that it is not calibrated from first principles, nor is it calibrated from geometric/parallax methods. Rather, SBF is currently being calibrated using (primarily) Cepheid and (a small number of) TRGB distances to galaxies close enough for those methods to provide a tie-in. For an extensive discussion of the systematic and random error differences between the three most recent determinations of the Hubble constant using SBF (as cited above, where the quoted systematic errors are comparable, but where the statistical errors differ by a factor of 3 or more) the interested reader is referred to [112].

The very strong intrinsic-color dependence of the SBF characteristic magnitude is assumed to be due to the effects of the metallicity distribution on the RGB colors, in combination with differing contributions of AGB stars due to different star formation histories. Uncrowded, high signal-to-noise color-magnitude diagrams of the stellar populations underwriting the SBF method would be important to have for a range of integrated colors in nearby elliptical galaxies so as to quantitatively constrain any potential systematic effects.

With *JWST*/*NIRCam* and other upcoming facilities, it will be possible to surmount the current 100 Mpc distance limit for SBF distances, perhaps taking it out to 300 Mpc, thus reducing the uncertainty from peculiar motions, as well as improving the statistical precision.

JCAP11(2023)050

8.2 Masers

H_2O mega-masers provide a powerful geometric tool for measuring extragalactic distances. These astrophysical masers, often found in the accretion disks around supermassive black holes, are akin to lasers, instead operating in the microwave regime. Water molecules in these disks amplify background radiation and produce coherent emission. The radial velocity shifts exhibited by the megamaser sources, observed with high-resolution radio interferometry, allow for the detailed mapping of the rotational dynamics of the maser-bearing accretion disk. By applying Kepler's laws to the derived rotation curve, the mass of the central supermassive black hole can be determined. A direct geometric distance to the galaxy can be obtained making use of the constrained orbital dynamics and precise angular measurements provided by Very Long Baseline Interferometry (VLBI) [113]. Allowing for warps and radial structure, the approximately Keplerian rotation curve for the disk can be modeled. The nearest and best-studied galaxy, NGC 4258, at a distance of about 7.5 Mpc, is too close to provide an independent measurement of the Hubble constant (i.e., free from local velocity-field perturbations) but it serves as a geometric anchor for the distance scale.

The *Megamaser Cosmology Project* has measured maser distances to 6 galaxies within 130 Mpc [114]. Adopting an average peculiar velocity uncertainty of ±250 km/s they determine a value of $H_0 = 73.9 \pm 3.0\,\mathrm{km\,s^{-1}\,Mpc^{-1}}$, with a range of values spanning 71.8 to $76.9\,\mathrm{km\,s^{-1}\,Mpc^{-1}}$, allowing for different means of correcting for peculiar velocities.

The maser method has the distinct advantage of offering a single-rung distance ladder (unlike SNe Ia), but the disadvantage that the numbers of galaxies for which this technique can be applied turns out to be very small (5 galaxies outside of the calibrator, NGC 4258). Hence, in terms of statistical precision, it will never rival SNe Ia (for which there are upwards of 1,000 host galaxies).

8.3 Strong gravitational lensing

Strong gravitational lensing offers an independent route for determining H_0 with the advantage that it can be carried out at cosmological distances (a one-step method), providing crucial cross-checks against measurements of the local distance scale and CMB measurements. In a gravitational lensing event, a massive foreground object (like a galaxy cluster) distorts the light from a background source (such as a more distant galaxy or quasar), resulting in multiple, often distorted, images of the source. The time delay between the arrival of light in these images, the "time-delay distance", is inversely proportional to the value of H_0, with a smaller dependence on Ω_m and Ω_Λ. Time-delay distances are derived by combining detailed modeling of the gravitational potential of the lens with precise measurements of the time delays between the multiple images [115, 116].

In practice, several key steps are involved in this method. First, high-quality imaging data of the lensing system must be obtained, most recently using HST or ground-based telescopes equipped with adaptive optics. These imaging data are then used to model the mass distribution of the lens, taking into account both luminous and dark matter components. In addition, photometric or spectroscopic monitoring of the background source is conducted to measure the time delays between the arrival of photons in the multiple images. This is a labor-intensive step, requiring observations over several months to years in order to accurately measure the variability and time delays [117].

JCAP11(2023)050

Advancements in lens modeling techniques and the quality of data are continually improving [118, 119]. Uncertainties in the gravitational lens method arise from the complexity of the lens model, whether the lens is located in a group or cluster, or whether there is mass along the line of sight, as well as due to the assumptions on the cosmological model. An inherent challenge for the method is the 'mass-sheet degeneracy', where an additional underlying mass density (mass sheet) can produce the same deflection angles and magnifications. Recently, a joint analysis of six gravitationally lensed quasars with measured time delays [119] resulted in a value of $H_0 = 73.3^{+1.7}_{-1.8}$ km/s/Mpc (a 2.4% uncertainty), assuming a flat ΛCDM cosmology. However, this result is dependent on assumptions about the mass-density radial distribution (e.g., a power-law mass profile) [120]. Dropping the assumptions about the mass profile, and instead using velocity dispersion measurements to break the mass-sheet degeneracy [121], the precision then drops to 8%, with $H_0 = 74.5^{+5.6}_{-6.1}$ km/s/Mpc. Additional imaging and spectroscopic data for 33 lenses then result in $H_0 = 67.4^{+4.1}_{-3.2}$ km/s/Mpc, improving the precision to 5%. It should be noted, however, that the profile constraints for the 33 lenses come from a different survey, with different sample selections (SLACS vs TDCOSMO).

Observations and analysis of the multiply lensed SN Refsdal result in values of $H_0 = 64^{+11}_{-9}\,\mathrm{km\,s^{-1}\,Mpc^{-1}}$ [122] and $64.8^{+4.4}_{-4.3}$, $66.6^{+4.1}_{-3.3}$, depending on the model adopted [123]. Lensed SNe Ia offer an advantage over lensed quasars due to the increased precision in the time delay measurements, as well as smaller uncertainties in the lens models.

Future improvements to this method will come with larger samples of lenses and measured time delays (to improve the statistical precision), for example, from the Vera Rubin Observatory, Euclid and the Nancy Grace Roman Observatory, and will require high signal-to-noise kinematic measurements to address the issue of the mass-sheet degeneracy, as well as detailed simulations [124].

8.4 Gravitational wave sirens

Inspiraling neutron star-neutron star binary systems have offered a new means of measuring H_0 that is completely independent of the local distance scale. In analogy with the astrophysical standard candles described earlier, the detection of gravitational waves from these systems provides a 'standard siren' that can be used to estimate the luminosity distance of the system out to cosmological distances, without the need for a local (astrophysical distance scale) calibration. The method requires both the detection of gravitational, as well as, electromagnetic radiation (the latter providing the redshift).

The method was first applied with stunning success to the event GW170817, located in a galaxy at 43 Mpc [125]. The authors determined a value of $H_0 = 70^{+12}_{-8}\,\mathrm{km\,s^{-1}\,Mpc^{-1}}$ (see figure 8). A number of factors contribute to the 15% uncertainty: detector noise, instrumental calibration uncertainties, uncertainty in the peculiar velocity of the host galaxy, and a geometrical factor dependent upon the covariance of distance with inclination angle. At a distance of 43 Mpc, the peculiar velocity is about 10% of the measured recessional velocity.

GW170817 was detected with high signal to noise almost immediately after LIGO was turned on in 2017. It led to the expectation that many more sources were likely to follow and that a value of H_0 to 2% accuracy would be possible by 2023 [126] with the detection of

JCAP11(2023)050

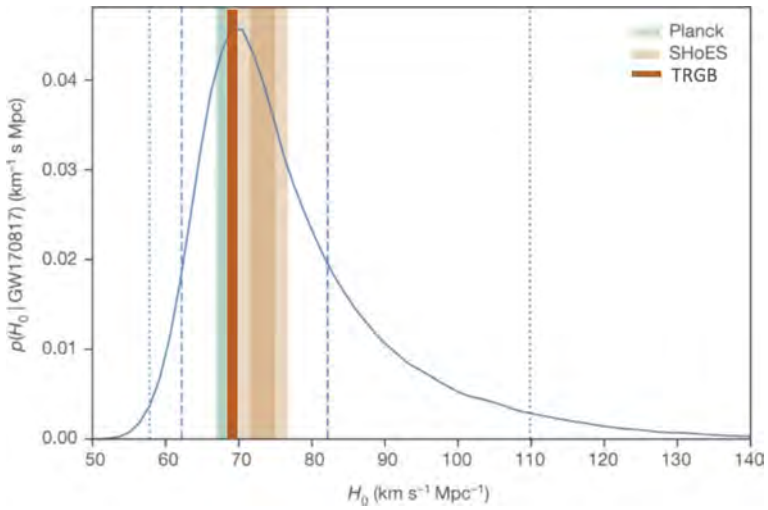

Figure 8. The marginalized posterior density distribution (blue line) for H_0 derived from the gravitational wave detection of GW170817. Constraints from Planck and *SHoES* are shown in green and orange, respectively. The TRGB value of $H_0 = 69\,\mathrm{km\,s^{-1}\,Mpc^{-1}}$ is shown in red. See text for details. Reproduced from [125], with permission from Springer Nature.

50 events, assuming that redshifts could be measured for each object. Sadly, as of summer, 2023, there have not yet been any comparable events, and an accurate measurement of H_0 with this technique will require patience. Ultimately, it will provide a critical independent means of comparison with the local distance scale.

9 The Hubble constant and the impact of the James Webb Space Telescope (JWST)

In this section, we provide an overview, as well as a current status report, of a new CCHP long-term program using *JWST*. This program is aimed at reducing the current systematics in the local extragalactic distance scale and the measurement of H_0. Specifically our goals are to: 1) exploit the high resolution of *JWST* to understand and reduce the possible effects of crowding and blending of Cepheids previously observed with HST, 2) improve the corrections for dust, 3) improve the constraints on the metallicity of Cepheids and 4) provide three independent measures (Cepheids, TRGB, JAGB) of the distances to the same galaxies, thereby reducing the overall systematic distance uncertainties. We note also the recent *JWST* results from [127] and [128] for NGC 1365, NGC 4258 and NGC 5584.

The blue sensitivity and high spatial resolution of HST made it an ideal facility for the discovery of Cepheid variables. At bluer (optical) wavelengths, the amplitudes of Cepheid variables are larger than at longer wavelengths due to the greater sensitivity of the surface brightness to temperature, thus facilitating their discovery [5]. HST's high resolution allowed Cepheids to be discovered in galaxies over a larger volume of space than could be accomplished from the ground, most recently out to distances of $\gtrsim$40 Mpc [9].

The superb science performance of *JWST* has greatly exceeded early expectations in terms of sensitivity, stability, image quality, as well as spectral range [129]. Two key features make *JWST* the optimal telescope for addressing the *accuracy* of measurements of H_0: its red

JCAP11(2023)050

sensitivity and higher spatial resolution. The extinction is significantly lower: A_J and $A_{[4.4]}$ are smaller by factors of 4 and 20× respectively, relative to the visual extinction, A_V; and factors of 2 and 10× lower relative to the I-band extinction A_I [130, 131]. *NIRCam* (F115W) imaging from *JWST* [132] has a sampling resolution four times that of HST *WFC*3 (F160W), with a FWHM of 0.04 arcsec on the former telescope and imager, versus 0.151 arcsec on the latter. In addition, in the near infrared (NIR), the objects that are causing contamination and crowding of the Cepheids are red giant and bright asymptotic giant branch stars, exacerbating crowding effects in the red, compared to optical wavelengths. *Importantly, with 4 times better resolution than HST, crowding effects are decreased by more than an order of magnitude in flux using* JWST.

We have been awarded time in Cycle 1 of *JWST* (JWST-GO-1995: P.I.W.L. Freedman; co-I B.F. Madore) to obtain observations of 10 nearby galaxies that are hosts to type SNe Ia, as well as observations of NGC 4258, a galaxy that provides an absolute calibration through its geometric distance based on H_2O megamasers (see sections 5.3, 8.2). There are three components to the program: three independent distances to each galaxy will be measured using Cepheids, the TRGB and *JAGB* stars, with a particular emphasis on testing for, and decreasing the systematic uncertainties that have often historically plagued distance scale determinations. The program is designed to deal specifically with known systematic effects in the measurement of distances to nearby galaxies: extinction and reddening by dust, metallicity effects and crowding/blending of stellar images. Simply getting more nearby galaxy distances (decreasing the statistical uncertainties) is insufficient to confirm or refute whether new physics beyond the standard cosmological model is required. At this time, systematic uncertainties are (and have historically always been) the dominant component of the error budget. Our goal is to decrease the systematic errors to the 2%-level, for each of the three methods.

The primary sample for the program is a subset of the nearest galaxies that have both reliable SN Ia photometry and previously-discovered Cepheid variables [5, 133], and for which TRGB and carbon-star distances can now also be measured. All three of these methods individually have high precision and can be independently used to calibrate SNe Ia. The observations are being carried out in the NIR at $F115W$ (or J band) and mid-infrared F356W at 3.6μm with the *JWST* Near-infrared Camera (*NIRCam*), and in parallel at $F115W$-band with the Near-infrared Imager and Slitless Spectrograph (*NIRISS*) [134]. Our first observations for NGC 7250 were carried out with the F444W filter at 4.4μm, but we have switched to F356W for the rest of the sample, owing to its higher sensitivity and better sampling. However, the F444W filter contains a CO bandhead that is sensitive to metallicity [135], and it is being used to carry out a test for metallicity effects in the galaxies, M101 and NGC 4258, as discussed further in section 9.1 below.

Our target fields were chosen to maximize inclusion of the largest possible number of known Cepheids in the inner disk, as well as the inclusion of the outer disk to detect carbon stars, and with a rotation angle optimized for the detection of halo red giants. The disk observations are being carried out with *NIRCam*; the outer halo observations with either *NIRCam* or parallel observations with *NIRISS*. We are carrying out the analysis using two independent software packages, DAOPHOT [136] and DOLPHOT [137], in order to provide a quantitative constraint on photometric errors that might arise due to differences in point-spread-function fitting in crowded fields.

JCAP11(2023)050

In brief, we find (1) The high-resolution *JWST* images of NGC 7250 demonstrate that many of the Cepheids observed with HST are significantly crowded by nearby neighbors. (2) The scatter in the *JWST* NIR Cepheid PL relation is decreased by a factor of two compared to those from HST. (3) The TRGB and carbon stars are well-resolved, and with the Cepheid measurements, will allow measurement of three independent distances to each of these galaxies. These new results illustrate the power of *JWST* to improve the measurement of extragalactic distances, and specifically, to address remaining systematics in the determination of H_0.

In figure 9 we show a color-magnitude diagram (F115W versus [F115W-F444W]) for the galaxy NGC 7250, which shows at a glance, the Cepheid instability strip, the position of the TRGB, the location of the JAGB stars, and the power of this three-in-one program. These three distance scales, all on a common photometric scale, contain valuable quantitative information as to potential systematic differences among the methods. The magnitudes are shown on an arbitrary scale, since at this stage of the analysis, the photometry is blinded. However, for the future calibration, the absolute flux calibration for *NIRCam* is nearing a level of 1%, down from its original 5% (M. Rieke, private communication); the absolute calibration will be tied to laboratory-standard measurements [138].

9.1 JWST Cepheid program

The *JWST* Cepheid sample for NGC 7250 was selected based on a completely new (end to end) re-analysis of the archival *SHoES* data [139]. This archival sample is comprised of 11 epochs of 'white light' (F350LP) photometry, with smaller numbers of (significantly lower signal-to-noise) phase points at three additional wavelengths (three at F555W, two at F814W and six at F160W). Periods and light curves were measured directly and independently using the F350LP photometry, using templates derived from well-measured Cepheids in the LMC [140]. Cepheid variable candidates were selected according to the following criteria: 1) optical colors consistent with known Cepheid variables; 2) optical amplitudes > 0.4 mag; 3) classified according to their light curve quality (requiring a classical 'saw-tooth' shape) at F350LP; 4) the light curves and images of the Cepheid candidates were independently inspected by eye by four team members. If there was disagreement about the quality of the candidate, it did not make the final cut; and 5) having no comparably bright nearby companions within the point spread function (PSF) at F350LP, as determined from the higher-resolution F115W data.[6] These stringent criteria were chosen to reduce the uncertainties due to crowding and low signal to noise. They result in a final sample of 16 uncrowded Cepheids with well-determined light curves. The photometry for all of the Cepheid candidate variables, both before and after final selection, will be made available on github [139].

The new *JWST* observations are allowing us to directly assess the degree to which crowding/blending effects have affected the (4× lower-resolution) HST photometry, on a star-by-star basis. In figure 10, we show multiband cutout images of eight Cepheids in NGC 7250 at a distance of 20 Mpc. From left to right are images at F350LP, F555W, and F814W (from HST) and F160W and F115W (from *JWST*). The cutouts are 2×2 arcsec on a side, and have been scaled as described in the figure caption. These images illustrate

[6] If the summed flux from resolved sources in the JWST F115W images within 4 NIRCAM pixels of the Cepheid candidate (0.124 arcsec or approximately one HST WFC3 IR pixel or 0.13 arcsec) was equal to or greater than the measured flux of the star itself, the candidate was considered to be crowded and not included in the final sample.

JCAP11(2023)050

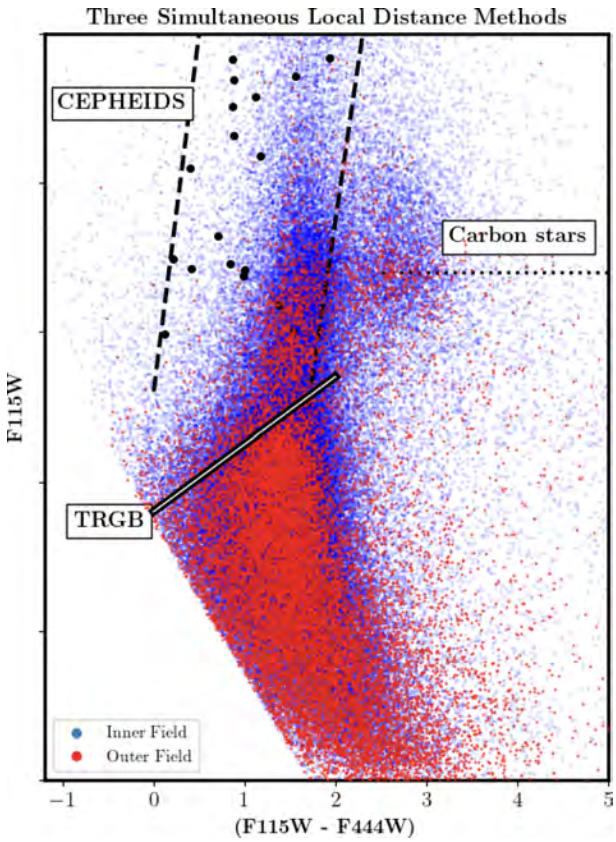

Figure 9. The relative disposition of the three stellar/astrophysical distance indicators, discussed in this review, seen plotted in a *JWST* F115W versus (F115-F444W) CMD. Cepheids are the black dots between the two vertical dashed lines, where the latter represent the red and blue limits of the instability strip. JAGB/Carbon stars are further to the red. Their mean luminosity is marked by the horizontal dotted line. Finally, the TRGB maximum J-band luminosity, as a function of color, is shown by the upward slanting yellow line at the top of the red giant branch at (F115W-F444W) $\approx$ 1.5 mag. See also figure 13.

the superb resolution and the power of *JWST* to improve the measurement of extragalactic distances. The effects of crowding, even in a galaxy as close as 20 Mpc are evident in this comparison. In the HST data, many of the Cepheid candidates are fainter than their nearby neighbors, rendering background subtraction challenging. *JWST* images for the complete sample of Cepheids in NGC 7250 are presented in [139].

In figure 11, we compare the Leavitt law for Cepheids in NGC 7250 observed with HST (left panel) and *JWST* (right panel). The *JWST* data are plotted on an arbitrary magnitude scale, as the data are still blinded. The slope is determined from the LMC, and restricted to log P $<$ 1.8, after which the period-luminosity relation in the LMC and other nearby galaxies (not shown) shows evidence for non-linearity. The scatter in the *JWST* F115W data for NGC 7250 is a factor of two smaller than the *SHoES* F160W data, which is all the more remarkable since the F115W data are for a single epoch only. In addition, a two-sigma rejection of candidates in the PL relation has been applied to the *SHoES* F160W data; no sigma cut has been applied to the *JWST* Cepheid candidates based on position in the PL relation.

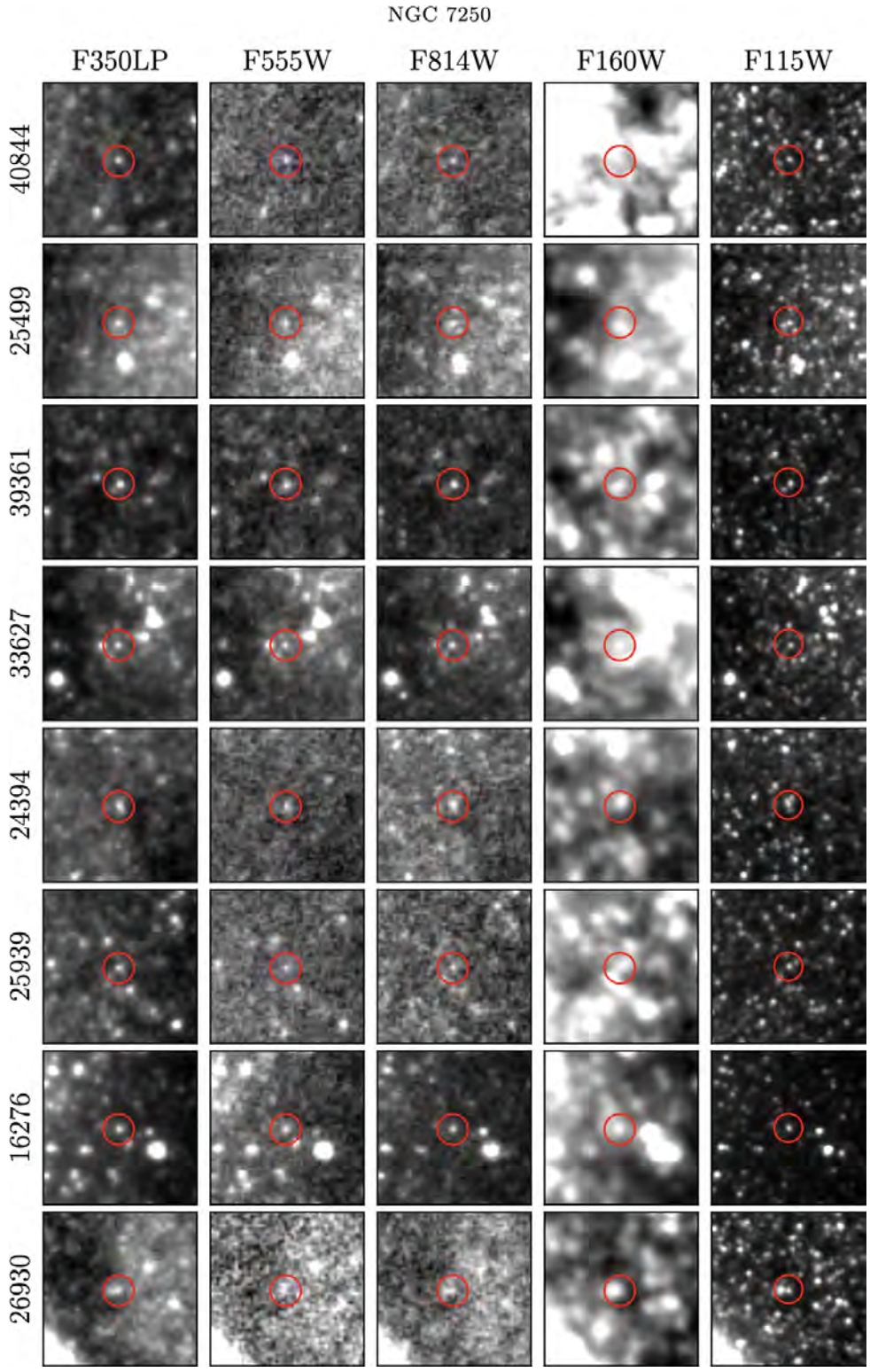

Figure 10. NGC 7250 Cepheids: a sample of cutout images for the light-curve-selected Cepheids in 5 photometric bands. Each cutout is 2 arcsec on a side. The red circles enclose the location of the Cepheid candidate and are 0.2 arcsec in radius. *JWST* J-band images are in the far right column. All other images (all four columns to the left) are from HST. Adapted from [139].

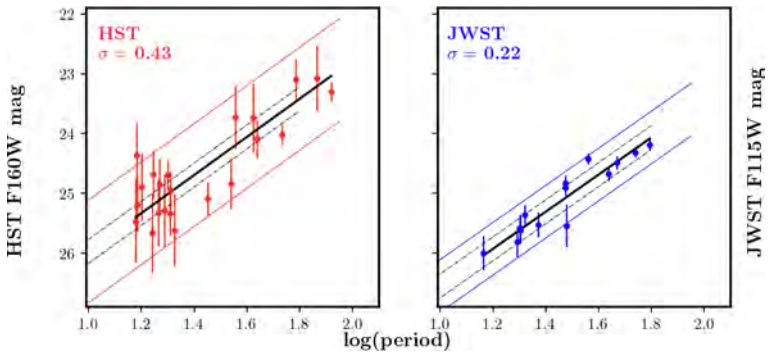

Figure 11. NIR Period-luminosity relations for Cepheids in NGC 7250. The left panel is HST F160W (H-band) data from the *SHoES* collaboration [9]; the right panel is JWST F115W (J-band) data from the CCHP [139]. The scatter about the period-luminosity fit in each filter is labeled in each plot.

When the data are unblinded, and an absolute calibration is established, the *JWST* data will allow us to also improve the accuracy of the reddening corrections to the individual galaxies and their Cepheids. A standard interstellar extinction curve [130, 131] can be fit to the multi-wavelength $F350, V, I, H$ and J-band apparent distance moduli [23, 60]. Finally, the 4.4μm-band can provide a direct and quantitative measure of the metallicity of the each of the Cepheids. *Spitzer* 4.5 μm observations of Cepheids in the Milky Way, the LMC and the SMC revealed a direct correlation between Cepheid metallicity and luminosity [135], a result of a CO bandhead that is present in the 4.4 μm filter. *JWST* observations across the disks of M101 and NGC 4258 have been scheduled as part of our program. In particular, there is a steep metallicity gradient in M101 [141], which will allow a direct test of the metallicity sensitivity at long wavelengths. The uncertainty due to the effects of metallicity remains one of the largest sources of systematic error in the Cepheid distance scale [81].

With improved reddening measurements, a direct measure of the metallicity, and a robust estimate of crowding/blending effects on current samples, we can address three of the largest sources of systematic uncertainty in the local Cepheid distance scale. The selection criteria adopted for inclusion in our final sample of Cepheids are deliberately conservative, with the intention of avoiding systematic effects due to crowding/blending, aiming for quality over quantity. The JWST data are still blinded, so in the future there will be a significant improvement to the distance measurements. However, near-IR photometry obtained using HST in this galaxy results in a larger scatter due to the lower spatial resolution and the lower signal to noise of the data.

We note that the recent study of NGC 5584 [128] finds a similar decrease in scatter of the *JWST* F150W (H-band) Leavitt law by a factor of 2.5 relative to that observed at F160W with HST. These authors find no evidence for a difference in H_0 that might be attributed to crowding effects based on the relative intercepts the Leavitt law for NGC 4258 and NGC 5584.

A larger sample of galaxies will ultimately reveal if crowding effects can finally be ruled out as a remaining source of uncertainty in the determination of H_0. It is important to keep in mind that crowding effects will become more severe with increasing distance. We note that 60% of the Riess et al. (2022) sample of galaxies in which Cepheids have been discovered lie at greater distances than NGC 7250 and NGC 5584 at 20 Mpc, and that 25% of the sample

JCAP11(2023)050

lies beyond 40 Mpc. At a distance of 40 Mpc, four times the area will be contained within a given pixel. For the most distant galaxy in the *SHoES* sample at 80 Mpc, 16 times the area will be covered. As the need for percent-level accuracy has grown, it remains important to demonstrate that crowding effects do not produce a systematic bias in the photometry and hence, the distance measurements for these more distant galaxies observed with HST.

9.2 JWST tip of the Red Giant Branch program

As noted in section 4, the TRGB provides one of the most precise and accurate means of measuring distances in the local universe [27]. The observed color-magnitude diagrams (CMDs) of the halos of nearby galaxies reveal a sharp discontinuity in the magnitude distribution of red giant branch stars at a well-determined luminosity, which corresponds to the location of the core helium-flash.

Measuring the TRGB in the near-IR has a number of advantages over the optical: 1) The extinction is significantly lower 2) TRGB stars are brighter in the NIR (M_J = –5.1 mag [39]) than in the optical (M_I = –4.05 mag [10]), making them comparable to that of Cepheids with periods of 10 days (M_J (10-day Cepheid) = –5.3 mag [26]). The slopes of the RGB as a function of wavelength are well-defined [29, 39, 40, 142]. 3) The peak luminosity of the giants occurs at NIR wavelengths. The disadvantage of the near-IR is that because the magnitude of the TRGB is no longer flat, as it is in the I-band, it necessitates more accurate measurements in a second filter to measure the slope of the RGB.

As part of our *JWST* CCHP program, the TRGB has been measured in NGC 4536, a galaxy located in the constellation Virgo, about 10 degrees south of the center of the Virgo Cluster. In figure 12 we show an $F814W$ versus [$F606W$-$F814W$] color magnitude diagram (CMD) [left panel] and $F115W$ versus [$F115W$-$F444W$] CMD [right panel] [143] for NGC 4536. The downward-arching black curve in the middle of the left panel illustrates the shallow color dependence of the TRGB at optical magnitudes [53]. The theoretically predicted slope of the infrared TRGB is also shown in black in the right panel. Also plotted are stellar evolutionary curves, as described in the figure caption. All magnitudes shown are on an arbitrary scale, but the two panels are aligned, illustrating the brighter magnitudes of the TRGB in the near-infrared relative to the optical. Once again, NGC 4258 will ultimately provide a geometric zero-point calibration. See [143] for details of the analysis of these data.

9.3 JWST resolved carbon-rich AGB stars program

In figure 13 we show an $F115W$ versus [$F115W - F444W$] CMD for the outer disk of the galaxy NGC 7250, which illustrates immediately the feasibility of using *JWST* and this method for distance determination. The carbon stars are located to the red of the TRGB, about one magnitude brighter than the tip, and exhibit a nearly-constant luminosity with a dispersion of only ±0.3 mag. These single-phase observations have only a slightly larger scatter than the intrinsic (time-averaged) scatter observed in the LMC [95]. Details of the analysis, as well as for the galaxies NGC 4536 and NGC 3972 are presented in [144].

JCAP11(2023)050

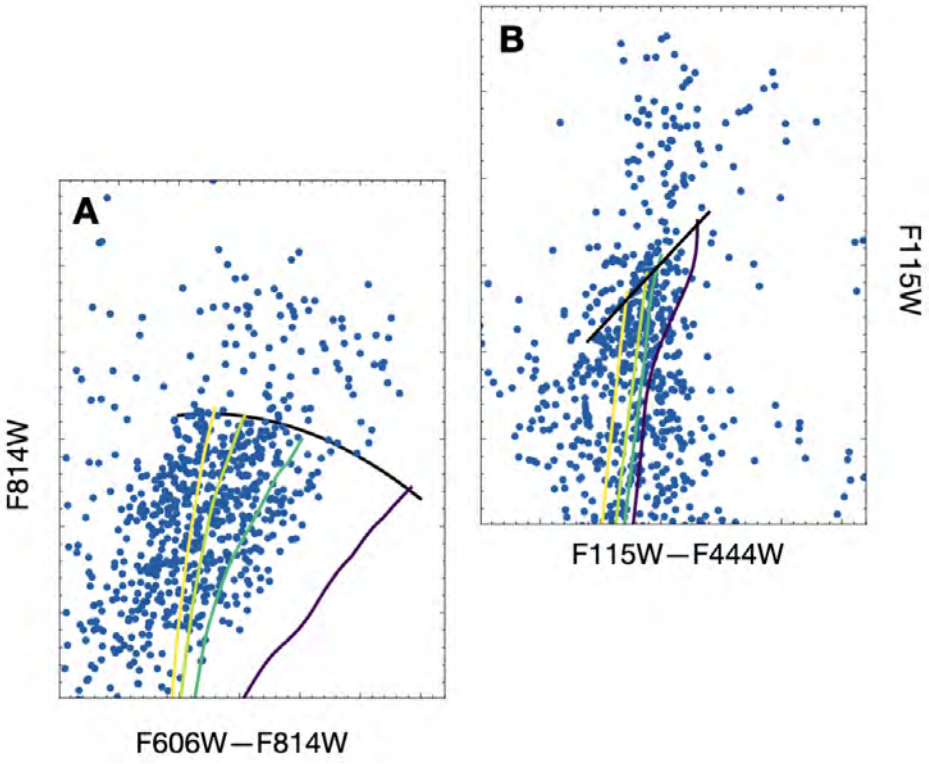

Figure 12. Optical HST (left) and near-infrared *JWST* (right) CMDs for stars located in the stellar halo of NGC 4536. The CMDs are aligned on their vertical axis to demonstrate the increasing brightness of RGB stars when observed in the infrared. The HST images represent a total of 14,000s in telescope exposure time, while the *JWST* images represent just 2,800s of exposure time. The known, shallow color dependence of the optical TRGB is overplotted on the left, while the theoretically-predicted slope of the infrared TRGB is overplotted on the right, both as black curves. In both CMDs, 10 Gyr theoretical stellar evolutionary tracks are shown and colored from light yellow to dark purple for metallicities Z = 0.002, 0.004, 0.008, and $Z_{\odot}$. The isochrones are shifted to terminate at the observed level of the TRGB.

10 Is there a crisis in cosmology?

Time will tell if cosmology is facing a crisis. It still remains at a crossroads [16]. The precision and accuracy with which extragalactic distances can be measured continue to improve, and many new facilities/programs are now either ongoing or will be online in the near future, which will lead to the continued refinement of the distance scale and to the measurement of H_0. In figure 14 we show a comparison of recently published values of H_0 from [88].

At this juncture, and given the still outstanding issues that need to be unambiguously addressed in order to allow a 1% measurement (e.g., small numbers of anchors, crowding effects, consistency across observing wavebands, metallicity effects), it is reasonable to keep an open mind as to the ultimate resolution of this latest crisis.

The current outstanding question essentially now revolves around '*the uncertainty in the uncertainty*'; i.e., have we yet reached a level of precision and accuracy in the local distance scale that can test the CMB model, which itself is quoted to have a precision exceeding

JCAP11(2023)050

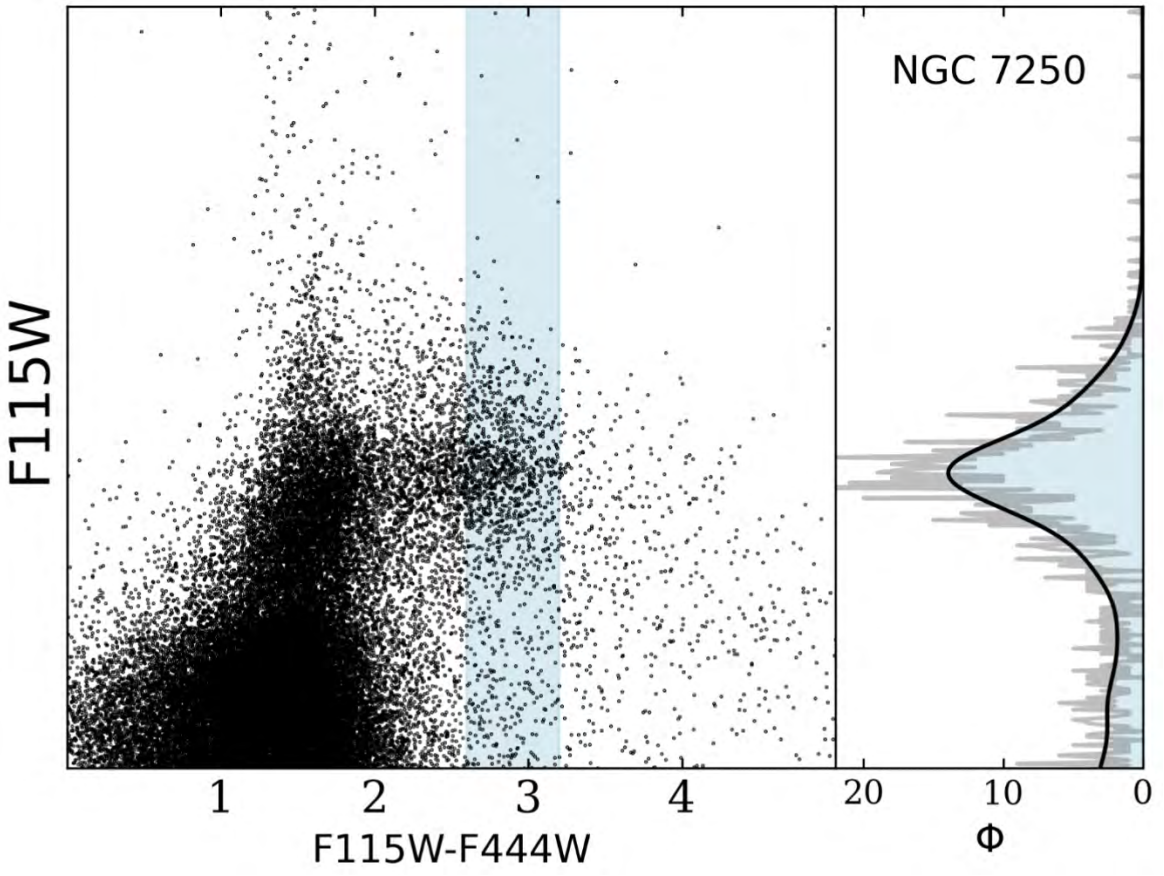

Figure 13. $F115W$ versus [$F115W$- $F444W$] color-magnitude diagram for the outer region of the galaxy NGC 7250 (left panel) from [144]. The JAGB stars were measured to be within the light blue shaded region. In the right-hand panel, the GLOESS-smoothed luminosity functions for the JAGB stars is shown in light blue, and the 0.01 mag binned luminosity functions are shown in grey. Within a window of 1.50 mag wide centered on the mode, the scatter of the JAGB stars is $\sigma = 0.32$ mag.

JCAP11(2023)050

1%. 5σ in experimental physics is the gold standard. How robust is the currently claimed astronomical 5σ result? If the result is secure at the 5–6σ level, then in principle, the question is settled, and no more work need be done. But the historical path en route to an accurate value of H_0 provides a cautionary tale of overcoming unrecognized systematic effects, so that extra scrutiny remains warranted. It is perhaps illustrative to consider that if the uncertainty in H_0 is currently underestimated by only a factor of 1.5, say, and $H_0 = 72.0 \pm 1.5\,\mathrm{km\,s^{-1}\,Mpc^{-1}}$, then the tension with the Planck results drops from 5σ to less than 3σ. Similarly if $H_0 = 72.0 \pm 2.0\,\mathrm{km\,s^{-1}\,Mpc^{-1}}$, the tension drops to 2σ.

Summary. The advancement in measuring the distances to galaxies over the past twenty-five years has been nothing short of remarkable. Just two decades ago, achieving accuracies within a few percent for the extragalactic distance scale was virtually unthinkable. This progress can be attributed to better detectors, increased wavelength coverage, innovative new, independent methods for measuring distances, and access to space, all of which have made it possible to address systematic effects including reddening/extinction from dust, metallicity, and crowding.

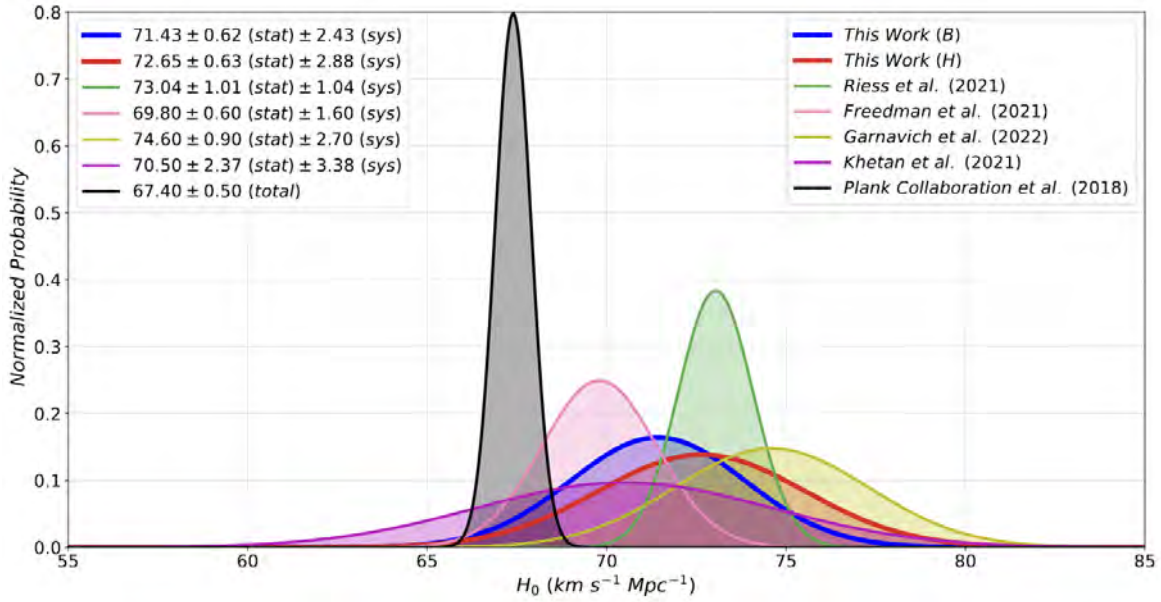

Figure 14. Probability distributions for H_0 for calibrations based on Cepheids [145], the TRGB [28] SBF from [88], compared to recent published values from the literature. The Planck Collaboration value from the CMB [14] shown in grey.

The launch of *JWST* has opened a new chapter in the measurement of extragalactic distances and H_0. The superb resolution and unequalled sensitivity at near-infrared wavelengths is already demonstrated in the first data from the nearby galaxies from two ongoing programs, including NGC 4258, NGC 7250, NGC 3972, NGC 5584 and NGC 4536, at distances out to 20 Mpc. These early data clearly demonstrate the promise of *JWST* for improving the measurement of extragalactic distances and the local, directly measured value of H_0. Our program has been optimized to observe Cepheids in the spiral arms of the inner disks of galaxies, JAGB stars in the extended disks, and TRGB stars in the outer halos of galaxies. All ten of the program galaxies are SN Ia hosts; an eleventh galaxy, NGC 4258, will provide an absolute distance calibration through the geometric measurement of its distance based on H_2O megamasers.

Although the measurements to local galaxies continue to improve, we need to keep open to the possibility that "unknown unknowns", or perhaps "known unknowns", could still be significant.[7] Keeping control of systematics below the 1% level (and convincing the community that this has been achieved) remains an immense challenge; one that will require the participation of several independent groups pursuing multiple independent methods. Such efforts are underway, and there is good reason to be optimistic that these efforts will converge and provide an answer to one of the most important problems in cosmology today — Is there new fundamental physics required beyond standard ΛCDM?

An augmented and extended version of this review can be found in the online version at https://arxiv.org/abs/2309.05618.

[7]With acknowledgement to Donald Rumsfeld who said "There are known knowns. These are things we know that we know. There are known unknowns. That is to say, there are things that we know we don't know. But there are also unknown unknowns. There are things we don't know we don't know".

JCAP11(2023)050

Acknowledgments

We thank our many students, postdocs, and collaborators over the last 40 years, all of whom contributed to much of the work described here, with particular thanks to Taylor Hoyt, In Sung Jang, Abigail Lee, Andy Monson, Kayla Owens, and Eric Persson. We thank Taylor Hoyt for figure 5, and for discussions of the H_0 tension. Thanks also to an anonymous referee who provided constructive comments that helped to improve the manuscript. We also thank the University of Chicago and the Carnegie Institution for Science for their support of this research.

This research is based in part on observations made with the NASA/ESA Hubble Space Telescope obtained from the Space Telescope Science Institute, which is operated by the Association of Universities for Research in Astronomy, Inc., under NASA contract NAS 5–26555. This work is also based in part on observations made with the NASA/ESA/CSA James Webb Space Telescope. The data were obtained from the Mikulski Archive for Space Telescopes at the Space Telescope Science Institute, which is operated by the Association of Universities for Research in Astronomy, Inc., under NASA contract NAS 5-03127. These observations are associated with HST programs #12880 and #14149 and with JWST program #1995. Financial support for this work was provided in part by NASA through HST program #16126 and JWST program #1995.

References

[1] H.S. Leavitt, *1777 variables in the Magellanic Clouds*, *Ann. Harvard Coll. Obs.* **60** (1908) 87.

[2] V.M. Slipher, *Spectrographic Observations of Nebulae*, *Pop. Astron.* **23** (1915) 21.

[3] E. Hubble, *A relation between distance and radial velocity among extra-galactic nebulae*, *Proc. Nat. Acad. Sci.* **15** (1929) 168 [INSPIRE].

[4] G. Lemaître, *Un Univers homogène de masse constante et de rayon croissant rendant compte de la vitesse radiale des nébuleuses extra-galactiques*, *Ann. Soc. Sci. Bruxelles* **47** (1927) 49.

[5] HST collaboration, *Final results from the Hubble Space Telescope key project to measure the Hubble constant*, *Astrophys. J.* **553** (2001) 47 [astro-ph/0012376] [INSPIRE].

[6] E. Di Valentino et al., *In the realm of the Hubble tension — a review of solutions*, *Class. Quant. Grav.* **38** (2021) 153001 [arXiv:2103.01183] [INSPIRE].

[7] W.L. Freedman et al., *Carnegie Hubble Program: A Mid-Infrared Calibration of the Hubble Constant*, *Astrophys. J.* **758** (2012) 24 [arXiv:1208.3281] [INSPIRE].

[8] A.G. Riess et al., *Large Magellanic Cloud Cepheid Standards Provide a 1% Foundation for the Determination of the Hubble Constant and Stronger Evidence for Physics beyond ΛCDM*, *Astrophys. J.* **876** (2019) 85 [arXiv:1903.07603] [INSPIRE].

[9] A.G. Riess et al., *A Comprehensive Measurement of the Local Value of the Hubble Constant with 1 km s^{-1} Mpc^{-1} Uncertainty from the Hubble Space Telescope and the SH0ES Team*, *Astrophys. J. Lett.* **934** (2022) L7 [arXiv:2112.04510] [INSPIRE].

[10] W.L. Freedman et al., *Calibration of the Tip of the Red Giant Branch (TRGB)*, arXiv:2002.01550 [DOI:10.3847/1538-4357/ab7339] [INSPIRE].

JCAP11(2023)050

[11] S. Dhawan et al., *A BayeSN distance ladder: H0 from a consistent modelling of Type Ia supernovae from the optical to the near-infrared*, *Mon. Not. Roy. Astron. Soc.* **524** (2023) 235 [arXiv:2211.07657] [INSPIRE].

[12] G.S. Anand et al., *Comparing Tip of the Red Giant Branch Distance Scales: An Independent Reduction of the Carnegie-Chicago Hubble Program and the Value of the Hubble Constant*, *Astrophys. J.* **932** (2022) 15 [arXiv:2108.00007] [INSPIRE].

[13] R.I. Anderson, *Young stellar distance indicators and the extragalactic distance scale*, arXiv:2302.14379 [INSPIRE].

[14] PLANCK collaboration, *Planck 2018 results. VI. Cosmological parameters*, *Astron. Astrophys.* **641** (2020) A6 [*Erratum ibid.* **652** (2021) C4] [arXiv:1807.06209] [INSPIRE].

[15] S. Yeung and M.-C. Chu, *Directional variations of cosmological parameters from the Planck CMB data*, *Phys. Rev. D* **105** (2022) 083508 [arXiv:2201.03799] [INSPIRE].

[16] W.L. Freedman, *Cosmology at a Crossroads*, *Nature Astron.* **1** (2017) 0121 [arXiv:1706.02739] [INSPIRE].

[17] M. López-Corredoira, *Hubble tensions: a historical statistical analysis*, *Mon. Not. Roy. Astron. Soc.* **517** (2022) 5805 [arXiv:2210.07078] [INSPIRE].

[18] B.F. Madore and W.L. Freedman, *Nonuniform Sampling and Periodic Signal Detection*, *Astrophys. J.* **630** (2005) 1054.

[19] C.R. Burns et al., *SN 2013aa and SN 2017cbv: Two Sibling Type Ia Supernovae in the spiral galaxy NGC 5643*, *Astrophys. J.* **895** (2020) 118 [arXiv:2004.13069] [INSPIRE].

[20] W.L. Freedman and B.F. Madore, *The Cepheid Extragalactic Distance Scale: Past, Present and Future*, arXiv:2308.02474 [INSPIRE].

[21] B.F. Madore and W.L. Freedman, *The Cepheid distance scale*, *Publ. Astron. Soc. Pac.* **103** (1991) 933 [INSPIRE].

[22] G. Bono, F. Caputo, M. Marconi and I. Musella, *Insights into the Cepheid distance scale*, *Astrophys. J.* **715** (2010) 277 [arXiv:1004.0363] [INSPIRE].

[23] W.L. Freedman and B.F. Madore, *The Hubble Constant*, *Ann. Rev. Astron. Astrophys.* **48** (2010) 673 [arXiv:1004.1856] [INSPIRE].

[24] D.G. Turner, *Classical Cepheids After 228 Years of Study*, *JAAVSO* **40** (2012) 502.

[25] L.M. Macri et al., *NICMOS observations of extragalactic Cepheids. 1. Photometry database and a test of the standard extinction law*, *Astrophys. J.* **549** (2001) 721 [astro-ph/0102125] [INSPIRE].

[26] S.E. Persson et al., *New Cepheid Period-Luminosity Relations for the Large Magellanic Cloud: 92 Near-Infrared Light Curves*, *Astron. J.* **128** (2004) 2239.

[27] W.L. Freedman et al., *The Carnegie-Chicago Hubble Program. VIII. An Independent Determination of the Hubble Constant Based on the Tip of the Red Giant Branch*, *Astrophys. J.* **882** (2019) 34 [arXiv:1907.05922] [INSPIRE].

[28] W.L. Freedman, *Measurements of the Hubble Constant: Tensions in Perspective*, *Astrophys. J.* **919** (2021) 16 [arXiv:2106.15656] [INSPIRE].

[29] B.F. Madore and W.L. Freedman, *Astrophysical Distance Scale: The AGB J-band Method. I. Calibration and a First Application*, *Astrophys. J.* **899** (2020) 66 [arXiv:2005.10792] [INSPIRE].

[30] W.L. Freedman and B.F. Madore, *Astrophysical Distance Scale II. Application of the JAGB Method: A Nearby Galaxy Sample*, *Astrophys. J.* **899** (2020) 67 [arXiv:2005.10793] [INSPIRE].

JCAP11(2023)050

[31] A.J. Lee et al., *The Astrophysical Distance Scale. III. Distance to the Local Group Galaxy WLM Using Multiwavelength Observations of the Tip of the Red Giant Branch, Cepheids, and JAGB Stars*, *Astrophys. J.* **907** (2021) 112 [arXiv:2012.04536] [INSPIRE].

[32] M.G. Lee, W.L. Freedman and B.F. Madore, *The Tip of the Red Giant Branch as a Distance Indicator for Resolved Galaxies*, *Astrophys. J.* **417** (1993) 553 [INSPIRE].

[33] L. Rizzi et al., *Tip of the Red Giant Branch Distances. 2. Zero-Point Calibration*, *Astrophys. J.* **661** (2007) 815 [astro-ph/0701518] [INSPIRE].

[34] M. Salaris, S. Cassisi and A. Weiss, *Red giant branch stars: the theoretical framework*, *Publ. Astron. Soc. Pac.* **114** (2002) 375 [astro-ph/0201387] [INSPIRE].

[35] B.F. Madore, V. Mager and W.L. Freedman, *Sharpening the Tip of the Red Giant Branch*, *Astrophys. J.* **690** (2009) 389 [arXiv:0809.2598] [INSPIRE].

[36] I.S. Jang et al., *The Carnegie-Chicago Hubble Program. IX. Calibration of the Tip of the Red Giant Branch Method in the Megamaser Host Galaxy, NGC 4258 (M106)*, *Astrophys. J.* **906** (2021) 125 [arXiv:2008.04181].

[37] J.J. Dalcanton et al., *Resolved Near-Infrared Stellar Populations in Nearby Galaxies*, *Astrophys. J. Suppl.* **198** (2012) 6 [arXiv:1109.6893] [INSPIRE].

[38] P.-F. Wu et al., *Infrared Tip of the Red Giant Branch and Distances to the Maffei/IC 342 Group*, *Astron. J.* **148** (2014) 7 [arXiv:1404.2987] [INSPIRE].

[39] B.F. Madore et al., *The Near-Infrared Tip of the Red Giant Branch. I. A Calibration in the Isolated Dwarf Galaxy IC 1613*, *Astrophys. J.* **858** (2018) 11 [arXiv:1803.01278] [INSPIRE].

[40] M.J. Durbin et al., *MCR-TRGB: A Multiwavelength-covariant, Robust Tip of the Red Giant Branch Measurement Method*, *Astrophys. J.* **898** (2020) 57 [arXiv:2006.08559].

[41] B.F. Madore and W.L. Freedman, *Helium Core Flash and Tip of RedGiant Branch Distances*, *ASP Conf. Ser.* **167** (1999) 161.

[42] B.F. Madore, W.L. Freedman, K.A. Owens and I.S. Jang, *Quantifying Uncertainties on the Tip of the Red Giant Branch Method*, *Astron. J.* **166** (2023) 2.

[43] M. Salaris and S. Cassisi, *The tip of the red giant branch as a distance indicator: results from evolutionary models*, *Mon. Not. Roy. Astron. Soc.* **289** (1997) 406 [astro-ph/9703186] [INSPIRE].

[44] M. Salaris and S. Cassisi, *Evolution of Stars and Stellar Populations*, John Wiley & Sons, Ltd (2005) [DOI:10.1002/0470033452].

[45] L. Bildsten, B. Paxton, K. Moore and P.J. Macias, *Acoustic Signatures of the Helium Core Flash*, *Astrophys. J. Lett.* **744** (2012) L6 [arXiv:1111.6867] [INSPIRE].

[46] R. Kippenhahn, A. Weigert and A. Weiss, *Stellar structure and evolution*, Springer (2012) [DOI:10.1007/978-3-642-30304-3] [INSPIRE].

[47] A. Serenelli et al., *The brightness of the red giant branch tip*, *Astron. Astrophys.* **606** (2017) A33 [arXiv:1706.09910].

[48] V.A. Mager, B.F. Madore and W.L. Freedman, *Metallicity-corrected Tip of the Red Giant Branch Distance to NGC 4258*, *Astrophys. J.* **689** (2008) 721 [arXiv:0808.2180] [INSPIRE].

[49] K. Krisciunas et al., *The Carnegie Supernova Project I: Third Photometry Data Release of Low-Redshift Type Ia Supernovae and Other White Dwarf Explosions*, *Astron. J.* **154** (2017) 211 [arXiv:1709.05146] [INSPIRE].

JCAP11(2023)050

[50] D. Scolnic et al., *Supercal: Cross-calibration of Multiple Photometric Systems to Improve Cosmological Measurements with Type Ia Supernovae*, *Astrophys. J.* **815** (2015) 117 [arXiv:1508.05361] [INSPIRE].

[51] T.J. Hoyt, *On Zero Point Calibration of the Red Giant Branch Tip in the Magellanic Clouds*, arXiv:2106.13337 [INSPIRE].

[52] G.S. Anand et al., *The Extragalactic Distance Database: The Color-Magnitude Diagrams/Tip of the Red Giant Branch Distance Catalog*, *Astron. J.* **162** (2021) 80 [arXiv:2104.02649].

[53] I.S. Jang and M.G. Lee, *The Tip of the Red Giant Branch Distances to Type Ia Supernova Host Galaxies. IV. Color Dependence and Zero-point Calibration*, *Astrophys. J.* **835** (2017) 28 [arXiv:1611.05040].

[54] D. Scolnic et al., *CATS: The Hubble Constant from Standardized TRGB and Type Ia Supernova Measurements*, *Astrophys. J. Lett.* **954** (2023) L31 [arXiv:2304.06693] [INSPIRE].

[55] F. Schweizer et al., *A New Distance to The Antennae Galaxies (NGC 4038/39) Based on the Type Ia Supernova 2007sr*, *Astron. J.* **136** (2008) 1482 [arXiv:0807.3955] [INSPIRE].

[56] I.S. Jang and M.G. Lee, *The Tip of the Red Giant Branch Distances to Type Ia Supernova Host Galaxies. III. NGC 4038/39 and NGC 5584*, *Astrophys. J.* **807** (2015) 133 [arXiv:1506.03089].

[57] B.F. Madore, W.L. Freedman, K.A. Owens and I.S. Jang, *Quantifying Uncertainties on the Tip of the Red Giant Branch Method*, *Astron. J.* **166** (2023) 2 [arXiv:2305.06195].

[58] CSP collaboration, *The Carnegie Supernova Project: Absolute Calibration and the Hubble Constant*, *Astrophys. J.* **869** (2018) 56 [arXiv:1809.06381] [INSPIRE].

[59] G. Pietrzyński et al., *A distance to the Large Magellanic Cloud that is precise to one per cent*, *Nature* **567** (2019) 200 [arXiv:1903.08096].

[60] A.J. Monson et al., *The Carnegie Hubble Program: The Leavitt Law at* 3.6 *and* 4.5 μm *in the Milky Way*, *Astrophys. J.* **759** (2012) 146 [arXiv:1209.4946] [INSPIRE].

[61] V. Scowcroft et al., *The Carnegie Hubble Program: The Leavitt Law at* 3.6 μm *and* 4.5 μm *in the Large Magellanic Cloud*, *Astrophys. J.* **743** (2011) 76 [*Erratum ibid.* **747** (2012) 8484] [arXiv:1108.4672] [INSPIRE].

[62] M.A.C. Perryman et al., *GAIA: Composition, formation and evolution of the Galaxy*, *Astron. Astrophys.* **369** (2001) 339 [astro-ph/0101235] [INSPIRE].

[63] G.F. Benedict et al., *Astrometry with hubble space telescope: a parallax of the fundamental distance calibrator delta cephei*, *Astron. J.* **124** (2002) 1695 [astro-ph/0206214] [INSPIRE].

[64] G.F. Benedict et al., *Hubble Space Telescope Fine Guidance Sensor Parallaxes of Galactic Cepheid Variable Stars: Period-Luminosity Relations*, *Astron. J.* **133** (2007) 1810 [*Erratum ibid.* **133** (2007) 2980] [astro-ph/0612465] [INSPIRE].

[65] G.F. Benedict et al., *Distance Scale Zero-Points from Galactic RR Lyrae Star Parallaxes*, *Astron. J.* **142** (2011) 187 [arXiv:1109.5631] [INSPIRE].

[66] L. Lindegren et al., *Gaia Early Data Release 3. Parallax bias versus magnitude, colour, and position*, *Astron. Astrophys.* **649** (2021) A4 [arXiv:2012.01742].

[67] L. Lindegren et al., *Gaia Early Data Release 3. The astrometric solution*, *Astron. Astrophys.* **649** (2021) A2 [arXiv:2012.03380].

[68] T. Cantat-Gaudin, *Milky Way Star Clusters and Gaia: A Review of the Ongoing Revolution*, *Universe* **8** (2022) 111.

[69] A.G.A. Brown et al., *Gaia Early Data Release 3. Summary of the contents and survey properties*, *Astron. Astrophys.* **649** (2021) A1 [arXiv:2012.01533].

JCAP11(2023)050

[70] L. Lindegren et al., *Gaia Data Release 1. Astrometry: one billion positions, two million proper motions and parallaxes*, *Astron. Astrophys.* **595** (2016) A4 [arXiv:1609.04303].

[71] L. Lindegren et al., *Gaia Data Release 2: The astrometric solution*, *Astron. Astrophys.* **616** (2018) A2 [arXiv:1804.09366] [INSPIRE].

[72] F. Arenou et al., *Gaia Data Release 2. Catalogue validation*, *Astron. Astrophys.* **616** (2018) A17 [arXiv:1804.09375] [INSPIRE].

[73] C.A.L. Bailer-Jones et al., *Estimating Distances from Parallaxes. V. Geometric and Photogeometric Distances to 1.47 Billion Stars in Gaia Early Data Release 3*, *Astron. J.* **161** (2021) 147 [arXiv:2012.05220].

[74] C. Fabricius et al., *Gaia Early Data Release 3. Catalogue validation*, *Astron. Astrophys.* **649** (2021) A5 [arXiv:2012.06242].

[75] K. El-Badry, H.-W. Rix and T.M. Heintz, *A million binaries from Gaia eDR3: sample selection and validation of Gaia parallax uncertainties*, *Mon. Not. Roy. Astron. Soc.* **506** (2021) 2269 [arXiv:2101.05282].

[76] K.A. Owens, W.L. Freedman, B.F. Madore and A.J. Lee, *Current Challenges in Cepheid Distance Calibrations Using Gaia Early Data Release 3*, *Astrophys. J.* **927** (2022) 8 [arXiv:2201.00733] [INSPIRE].

[77] M.C. Reyes and R.I. Anderson, *A 0.9% calibration of the Galactic Cepheid luminosity scale based on Gaia DR3 data of open clusters and Cepheids*, *Astron. Astrophys.* **672** (2023) A85 [arXiv:2208.09403] [INSPIRE].

[78] E.M.L. Humphreys et al., *Toward a New Geometric Distance to the Active Galaxy NGC 4258. III. Final Results and the Hubble Constant*, *Astrophys. J.* **775** (2013) 13 [arXiv:1307.6031] [INSPIRE].

[79] M.J. Reid, D.W. Pesce and A.G. Riess, *An Improved Distance to NGC 4258 and its Implications for the Hubble Constant*, *Astrophys. J. Lett.* **886** (2019) L27 [arXiv:1908.05625] [INSPIRE].

[80] T.J. Hoyt, *Sub-per-cent determination of the brightness at the tip of the red giant branch in the Magellanic Clouds*, *Nature Astron.* **7** (2023) 590.

[81] G. Efstathiou, *A Lockdown Perspective on the Hubble Tension (with comments from the SH0ES team)*, arXiv:2007.10716 [INSPIRE].

[82] D. Brout et al., *The Pantheon+ Analysis: Cosmological Constraints*, *Astrophys. J.* **938** (2022) 110 [arXiv:2202.04077] [INSPIRE].

[83] C. Contreras et al., *The Carnegie Supernova Project: First Photometry Data Release of Low-Redshift Type Ia Supernovae*, *Astron. J.* **139** (2010) 519 [arXiv:0910.3330] [INSPIRE].

[84] G. Folatelli et al., *Spectroscopy of Type Ia Supernovae by the Carnegie Supernova Project*, *Astrophys. J.* **773** (2013) 53 [arXiv:1305.6997] [INSPIRE].

[85] M.M. Phillips et al., *Carnegie Supernova Project-II: Extending the Near-infrared Hubble Diagram for Type Ia Supernovae to $z \sim 0.1$*, *Publ. Astron. Soc. Pac.* **131** (2018) 014001 [arXiv:1810.09252] [INSPIRE].

[86] E.Y. Hsiao et al., *Carnegie Supernova Project-II: The Near-infrared Spectroscopy Program*, *Publ. Astron. Soc. Pac.* **131** (2018) 014002 [arXiv:1810.08213].

[87] A.G. Riess et al., *A 2.4% Determination of the Local Value of the Hubble Constant*, *Astrophys. J.* **826** (2016) 56 [arXiv:1604.01424] [INSPIRE].

[88] S.A. Uddin et al., *Carnegie Supernova Project-I and -II: Measurements of H_0 using Cepheid, TRGB, and SBF Distance Calibration to Type Ia Supernovae*, arXiv:2308.01875 [INSPIRE].

JCAP11(2023)050

[89] D. Scolnic et al., *The Pantheon+ Analysis: The Full Data Set and Light-curve Release*, *Astrophys. J.* **938** (2022) 113 [arXiv:2112.03863] [INSPIRE].

[90] PAN-STARRS1 collaboration, *The Complete Light-curve Sample of Spectroscopically Confirmed SNe Ia from Pan-STARRS1 and Cosmological Constraints from the Combined Pantheon Sample*, *Astrophys. J.* **859** (2018) 101 [arXiv:1710.00845] [INSPIRE].

[91] SDSS collaboration, *Improved cosmological constraints from a joint analysis of the SDSS-II and SNLS supernova samples*, *Astron. Astrophys.* **568** (2014) A22 [arXiv:1401.4064] [INSPIRE].

[92] LSST collaboration, *LSST: from Science Drivers to Reference Design and Anticipated Data Products*, *Astrophys. J.* **873** (2019) 111 [arXiv:0805.2366] [INSPIRE].

[93] R. Hounsell et al., *Simulations of the WFIRST Supernova Survey and Forecasts of Cosmological Constraints*, *Astrophys. J.* **867** (2018) 23 [arXiv:1702.01747] [INSPIRE].

[94] S. Nikolaev and M.D. Weinberg, *Stellar populations in the large magellanic cloud from 2mass*, *Astrophys. J.* **542** (2000) 804 [astro-ph/0003012] [INSPIRE].

[95] M.D. Weinberg and S. Nikolaev, *Structure of the large magellanic cloud from 2mass*, *Astrophys. J.* **548** (2001) 712 [astro-ph/0003204] [INSPIRE].

[96] P. Ripoche, J. Heyl, J. Parada and H. Richer, *Carbon stars as standard candles: I. The luminosity function of carbon stars in the Magellanic Clouds*, *Mon. Not. Roy. Astron. Soc.* **495** (2020) 2858 [arXiv:2005.05539].

[97] A.J. Lee et al., *The Astrophysical Distance Scale. V. A 2% Distance to the Local Group Spiral M33 via the JAGB Method, Tip of the Red Giant Branch, and Leavitt Law*, *Astrophys. J.* **933** (2022) 201 [arXiv:2205.11323] [INSPIRE].

[98] A.J. Lee, *Carbon Stars as Standard Candles: An Empirical Test for the Reddening, Metallicity, and Age Sensitivity of the J-region Asymptotic Giant Branch (JAGB) Method*, *Astrophys. J.* **956** (2023) 15 [arXiv:2305.02453] [INSPIRE].

[99] B. Zgirski et al., *The Araucaria Project. Distances to Nine Galaxies Based on a Statistical Analysis of their Carbon Stars (JAGB Method)*, *Astrophys. J.* **916** (2021) 19.

[100] P. Marigo et al., *A New Generation of PARSEC-COLIBRI Stellar Isochrones Including the TP-AGB Phase*, *Astrophys. J.* **835** (2017) 77 [arXiv:1701.08510].

[101] M. Salaris et al., *Detailed AGB evolutionary models and near-infrared colours of intermediate-age stellar populations: tests on star clusters*, *Astron. Astrophys.* **565** (2014) A9 [arXiv:1403.2505].

[102] G. Pastorelli et al., *Constraining the thermally pulsing asymptotic giant branch phase with resolved stellar populations in the Large Magellanic Cloud*, *Mon. Not. Roy. Astron. Soc.* **498** (2020) 3283 [arXiv:2008.08595].

[103] I. Iben Jr. and A. Renzini, *Asymptotic giant branch evolution and beyond*, *Ann. Rev. Astron. Astrophys.* **21** (1983) 271 [INSPIRE].

[104] F. Herwig, *Evolution of Solar and Intermediate-Mass Stars*, in *Planets, Stars and Stellar Systems*, Springer Netherlands (2013), p. 397–445 [DOI:10.1007/978-94-007-5615-1_8].

[105] H.J. Habing and H. Olofsson, *AGB Stars: History, Structure, and Characteristics*, in *Astronomy and Astrophysics Library*, Springer New York (2004), p. 1–21 [DOI:10.1007/978-1-4757-3876-6_1].

[106] P. Marigo et al., *A Fresh Look at AGB Stars in Galactic Open Clusters with Gaia: Impact on Stellar Models and the Initial-Final Mass Relation*, *Astrophys. J. Suppl.* **258** (2022) 43 [arXiv:2111.03527].

[107] A.I. Boothroyd, I.-J. Sackmann and S.C. Ahern, *Prevention of High-Luminosity Carbon Stars by Hot Bottom Burning*, *Astrophys. J.* **416** (1993) 762.

JCAP11(2023)050

[108] J. Tonry and D.P. Schneider, *A new technique for measuring extragalactic distances*, *Astron. J.* **96** (1988) 807.

[109] M. Cantiello and J.P. Blakeslee, *Surface Brightness Fluctuations*, arXiv:2307.03116 [INSPIRE].

[110] J.P. Blakeslee et al., *The Hubble Constant from Infrared Surface Brightness Fluctuation Distances*, *Astrophys. J.* **911** (2021) 65 [arXiv:2101.02221] [INSPIRE].

[111] N. Khetan et al., *A new measurement of the Hubble constant using Type Ia supernovae calibrated with surface brightness fluctuations*, *Astron. Astrophys.* **647** (2021) A72 [arXiv:2008.07754] [INSPIRE].

[112] P. Garnavich et al., *Connecting Infrared Surface Brightness Fluctuation Distances to Type Ia Supernova Hosts: Testing the Top Rung of the Distance Ladder*, *Astrophys. J.* **953** (2023) 35 [arXiv:2204.12060] [INSPIRE].

[113] K.Y. Lo, *Mega-Masers and Galaxies*, *Ann. Rev. Astron. Astrophys.* **43** (2005) 625.

[114] D.W. Pesce et al., *The Megamaser Cosmology Project. XIII. Combined Hubble constant constraints*, *Astrophys. J. Lett.* **891** (2020) L1 [arXiv:2001.09213] [INSPIRE].

[115] S. Refsdal, *On the possibility of determining Hubble's parameter and the masses of galaxies from the gravitational lens effect*, *Mon. Not. Roy. Astron. Soc.* **128** (1964) 307 [INSPIRE].

[116] R. Blandford and R. Narayan, *Fermat's principle, caustics, and the classification of gravitational lens images*, *Astrophys. J.* **310** (1986) 568 [INSPIRE].

[117] DES collaboration, *COSMOGRAIL: the COSmological MOnitoring of GRAvItational Lenses — XVI. Time delays for the quadruply imaged quasar DES J0408−5354 with high-cadence photometric monitoring*, *Astron. Astrophys.* **609** (2018) A71 [arXiv:1706.09424] [INSPIRE].

[118] S.H. Suyu et al., *H0LiCOW — I. H0 Lenses in COSMOGRAIL's Wellspring: program overview*, *Mon. Not. Roy. Astron. Soc.* **468** (2017) 2590 [arXiv:1607.00017] [INSPIRE].

[119] K.C. Wong et al., *H0LiCOW — XIII. A 2.4 per cent measurement of H0 from lensed quasars: 5.3σ tension between early- and late-Universe probes*, *Mon. Not. Roy. Astron. Soc.* **498** (2020) 1420 [arXiv:1907.04869] [INSPIRE].

[120] S. Birrer and T. Treu, *TDCOSMO — V. Strategies for precise and accurate measurements of the Hubble constant with strong lensing*, *Astron. Astrophys.* **649** (2021) A61 [arXiv:2008.06157] [INSPIRE].

[121] S. Birrer et al., *TDCOSMO — IV. Hierarchical time-delay cosmography — joint inference of the Hubble constant and galaxy density profiles*, *Astron. Astrophys.* **643** (2020) A165 [arXiv:2007.02941] [INSPIRE].

[122] J. Vega-Ferrero, J.M. Diego, V. Miranda and G.M. Bernstein, *The Hubble constant from SN Refsdal*, *Astrophys. J. Lett.* **853** (2018) L31 [arXiv:1712.05800] [INSPIRE].

[123] P.L. Kelly et al., *Constraints on the Hubble constant from supernova Refsdal's reappearance*, *Science* **380** (2023) abh1322 [arXiv:2305.06367] [INSPIRE].

[124] X. Ding et al., *Time delay lens modelling challenge*, *Mon. Not. Roy. Astron. Soc.* **503** (2021) 1096 [arXiv:2006.08619] [INSPIRE].

[125] LIGO SCIENTIFIC et al. collaborations, *A gravitational-wave standard siren measurement of the Hubble constant*, *Nature* **551** (2017) 85 [arXiv:1710.05835] [INSPIRE].

[126] H.-Y. Chen, M. Fishbach and D.E. Holz, *A two per cent Hubble constant measurement from standard sirens within five years*, *Nature* **562** (2018) 545 [arXiv:1712.06531] [INSPIRE].

[127] W. Yuan, A.G. Riess, S. Casertano and L.M. Macri, *A First Look at Cepheids in a Type Ia Supernova Host with JWST*, *Astrophys. J. Lett.* **940** (2022) L17 [arXiv:2209.09101] [INSPIRE].

JCAP11(2023)050

[128] A.G. Riess et al., *Crowded No More: The Accuracy of the Hubble Constant Tested with High-resolution Observations of Cepheids by JWST*, *Astrophys. J. Lett.* **956** (2023) L18 [arXiv:2307.15806] [INSPIRE].

[129] J. Rigby et al., *The Science Performance of JWST as Characterized in Commissioning*, arXiv:2207.05632 [DOI:10.1088/1538-3873/acb293].

[130] J.A. Cardelli, G.C. Clayton and J.S. Mathis, *The relationship between infrared, optical, and ultraviolet extinction*, *Astrophys. J.* **345** (1989) 245 [INSPIRE].

[131] R. Indebetouw et al., *The Wavelength Dependence of Interstellar Extinction from* 1.25 *to* 8.0 μm *Using GLIMPSE Data*, *Astrophys. J.* **619** (2005) 931 [astro-ph/0406403] [INSPIRE].

[132] M.J. Rieke et al., *Performance of NIRCam on JWST in Flight*, *Publ. Astron. Soc. Pac.* **135** (2023) 028001.

[133] A.G. Riess et al., *The Accuracy of the Hubble Constant Measurement Verified through Cepheid Amplitudes*, *Astrophys. J. Lett.* **896** (2020) L43 [arXiv:2005.02445] [INSPIRE].

[134] C.J. Willott et al., *The Near-infrared Imager and Slitless Spectrograph for the James Webb Space Telescope. II. Wide Field Slitless Spectroscopy*, *Publ. Astron. Soc. Pac.* **134** (2022) 025002 [arXiv:2202.01714].

[135] V. Scowcroft et al., *The Carnegie Chicago Hubble Program: The Mid-Infrared Colours of Cepheids and the Effect of Metallicity on the CO Band-head at* 4.6 μm, *Mon. Not. Roy. Astron. Soc.* **459** (2016) 1170 [arXiv:1603.03776].

[136] P.B. Stetson, *DAOPHOT — A computer program for crowded field stellar photometry*, *Publ. Astron. Soc. Pac.* **99** (1987) 191 [INSPIRE].

[137] D.R. Weisz et al., *The JWST Resolved Stellar Populations Early Release Science Program II. Survey Overview*, arXiv:2301.04659 [DOI:10.48550/ARXIV.2301.04659].

[138] K.D. Gordon et al., *The James Webb Space Telescope Absolute Flux Calibration. I. Program Design and Calibrator Stars*, *Astron. J.* **163** (2022) 267 [arXiv:2204.06500].

[139] K. Owens et al., *Resolving the Extragalactic Distance Scale with JWST: Cepheids in NGC 7250*, submitted to *Astrophys. J.* (2023).

[140] K. Owens et al., *Template Fitting for Cepheid Variables*, in preparation.

[141] R. Garner et al., *Deep Narrowband Photometry of the M101 Group: Strong-line Abundances of 720 H ii Regions*, *Astrophys. J.* **941** (2022) 182 [arXiv:2211.07463].

[142] T.J. Hoyt et al., *The Near-Infrared Tip of the Red Giant Branch. II. An Absolute Calibration in the Large Magellanic Cloud*, *Astrophys. J.* **858** (2018) 12 [arXiv:1803.01277] [INSPIRE].

[143] T. Hoyt et al., *Simultaneous JWST Imaging of Multiple Distance Indicators in NGC 4536: A Successful Detection and Measurement of the Infrared Tip of the Red Giant Branch*, submitted to *Astrophys. J.* (2023).

[144] A. Lee et al., *First JWST Observations of JAGB Stars in the SN Ia Host Galaxies: NGC 7250, NGC 4536, NGC 3972*, submitted to *Astrophys. J.* (2023).

[145] A.G. Riess et al., *Cosmic Distances Calibrated to 1% Precision with Gaia EDR3 Parallaxes and Hubble Space Telescope Photometry of 75 Milky Way Cepheids Confirm Tension with* Λ*CDM*, *Astrophys. J. Lett.* **908** (2021) L6 [arXiv:2012.08534] [INSPIRE].

JCAP11(2023)050